AD-A102 106 SCIENCE APPLICATIONS INC MONTEREY CA F/G 4/2
TROPICAL CYCLONE WIND PROBABILITY FORECASTING (WINDP).(U)
APR 81 J D JARRELL N00228-78-C-3337
UNCLASSIFIED NEPRF-CR-81-03 NL

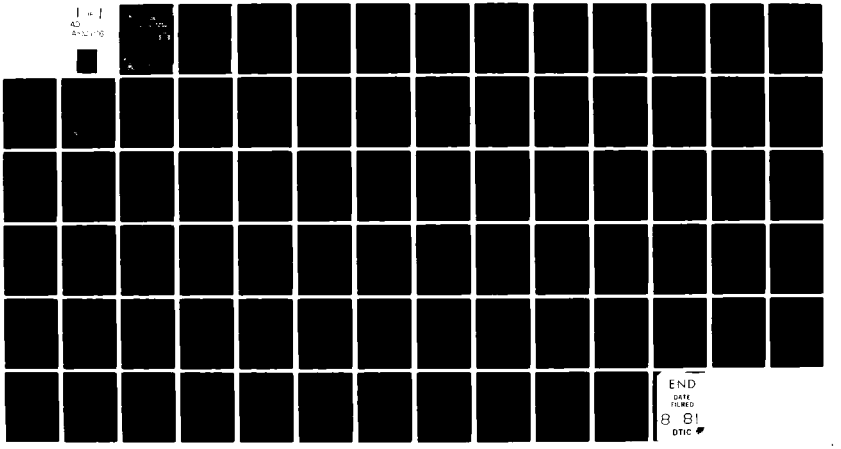

END
DATE FILMED
8 81
DTIC

NAVENVPREDRSCHFAC
CONTRACTOR REPORT
CR 81-03

LEVEL II

12

TROPICAL CYCLONE WIND PROBABILITY FORECASTING (WINDP)

Prepared By:

Jerry D. Jarrell
Science Applications, Inc.
Monterey, CA 93940

Contract No. N00228-78-C-3337

APRIL 1981

Prepared For:
NAVAL ENVIRONMENTAL PREDICTION RESEARCH FACILITY
MONTEREY, CALIFORNIA 93940

UNCLASSIFIED

SECURITY CLASSIFICATION OF THIS PAGE (When Data Entered)

REPORT DOCUMENTATION PAGE

READ INSTRUCTIONS BEFORE COMPLETING FORM

REPORT NUMBER: NAVENVPREDRSCHFAC Contractor Report CR 81-03	2. GOVT ACCESSION NO. / 3. RECIPIENT'S CATALOG NUMBER
4. TITLE (and Subtitle): Tropical Cyclone Wind Probability Forecasting (WINDP)	5. TYPE OF REPORT & PERIOD COVERED: Final Rept.
	6. PERFORMING ORG. REPORT NUMBER
7. AUTHOR(s): Jerry D. Jarrell	8. CONTRACT OR GRANT NUMBER(s): N00228-78-C-3337
9. PERFORMING ORGANIZATION NAME AND ADDRESS: Science Applications, Inc. (SAI), 1999 Monterey-Salinas Highway, Monterey, CA 93940	10. PROGRAM ELEMENT, PROJECT, TASK AREA & WORK UNIT NUMBERS: PE 63207N PN 7W0513, NEPRF WU 6.3-14
11. CONTROLLING OFFICE NAME AND ADDRESS: Naval Air Systems Command, Department of the Navy, Washington, DC 20361	12. REPORT DATE: April 1981
	13. NUMBER OF PAGES: 70
14. MONITORING AGENCY NAME & ADDRESS (if different from Controlling Office): Naval Environmental Prediction Research Facility, Monterey, CA 93940	15. SECURITY CLASS. (of this report): UNCLASSIFIED
	15a. DECLASSIFICATION/DOWNGRADING SCHEDULE

16. DISTRIBUTION STATEMENT (of this Report)

Approved for public release; distribution unlimited

17. DISTRIBUTION STATEMENT (of the abstract entered in Block 20, if different from Report)

18. SUPPLEMENTARY NOTES

19. KEY WORDS (Continue on reverse side if necessary and identify by block number)

Tropical cyclone
Typhoon
Hurricane
Wind probability

20. ABSTRACT (Continue on reverse side if necessary and identify by block number)

The development of a model to estimate 30 and 50 kt wind probabilities from tropical cyclone forecasts is described. Some examples to illustrate the use of probabilities are discussed.

The model is based on position forecast errors, which are used to determine the probability of a cyclone occupying a particular geographical position, and on wind profile errors. Wind profile errors consist of errors in the forecast maximum wind and errors in the forecast radius of 30 and 50 kt winds. The profile errors are used to estimate the probability of (continued on reverse)

DD FORM 1 JAN 73 1473 EDITION OF 1 NOV 65 IS OBSOLETE
S/N 0102-014-6601

UNCLASSIFIED

SECURITY CLASSIFICATION OF THIS PAGE (When Data Entered)

Abstract, Block 20, Continued

30 and 50 kt winds occurring at a point, given that the cyclone occupies a particular position. These position and wind probability elements are combined by using an assumption of independence which is supported by correlation coefficients.

The model, which includes features of the earlier strike probability model, is tested on independent data. Test results are shown to illustrate good agreement between forecast probability and the frequency of occurrence of 30 and 50 kt winds.

TABLE OF CONTENTS

INTRODUCTION

The concepts of tropical cyclone wind probability are an extension of the strike probability concepts. The latter are described by Jarrell in NAVENVPREDRSCHFAC contractor report CR78-01 and will only be summarized herein.

Strike probability is a means of inferring from a tropical cyclone forecast the probability that the cyclone center will be within an area at a specific time or will pass through that area within some time interval.

The theory of strike probability is based on the following assumptions:

(a) That all forecasts are subject to error;
(b) That some forecasts are more difficult than others and therefore will likely result in a larger error; and
(c) That error occurrence is random so as to approximate a bivariate normal probability distribution (normal in both N-S and E-W directions).

A study by Nicklin (1977) of western North Pacific tropical cyclone track forecast errors confirmed the soundness of these assumptions and provided a method to distinguish forecasts of average difficulty from easy and difficult forecasts. Nicklin also provided sufficient statistical parameters to describe the bivariate normal distributions for each of three classes and for nowcasts and forecasts of 24, 48 and 72 hour length.

The strike probability program, now in an operational status at the Fleet Numerical Oceanography Center (FNOC), has been well received. Its major limitation is that its use requires that the distance between a passing tropical cyclone and a station or geographic point be of some assumed significance. This usually requires the assumption that if the cyclone passes within x nautical miles of a station, winds of at least v knots will be observed and that otherwise those velocities would not occur. Wind probability somewhat removes this requirement by directly estimating the probabilities for the two cases of the winds being at least 30 and at least 50 knots. Wind probability, then, represents an additional refinement to the strike probability program but since the original concepts allow user flexibility they will remain an important part of the package.

In the pages that follow the wind probability program will be described. The format will be two-tiered with user oriented descriptive material in the first sections and more technical material in the last section. This design permits relatively light reading which will sufficiently describe the use of the model for most users without wading through the whys. The purpose of the technical section is to provide indepth information sufficient to describe the assumptions made, and some indications as to how critical and how good these assumptions are. This kind of information better equips the user with an appreciation of the precision of the output numbers and the conditions under which the information is likely to be most (or least) representative.

Section 1

DESCRIPTIVE SECTION

1.1 Probability: General

The probability of some event occurring is often used as a guage of the risk involved. Suppose the probability of a person being struck by lightning on a particular stormy day was estimated to be 1 in 1 million. This does not mean he will not be struck, although we certainly consider it unlikely. It does not mean he will be hit by .000001 lightning bolts since fractional parts of a lightning bolt do not exist. It does not mean the probability of his being hit is 0.000001, for the real probability can only be 1.0 or 0.0, and can only be known after the fact. It is, however, an estimate of that portion of like cases (man stands in rain) in which the event (he gets struck) is likely to occur.

For descriptive material, this may appear to be an unnecessary technicality but it is vital that this be understood. What we call probabilities are always estimates. When we use a normal (or some other) statistical distribution, remember we have only made an approximation. The proof of its goodness is how reasonable are the estimates of probability over the long haul. To test reasonableness we usually use some sort of a statistical test over a large number of cases. In this paper the normal assumption is invoked several places. We try to minimize the risk that this assumption is inappropriate by being selective and only applying it where it at least appears appropriate.

1.1.1 Why Probability?

Tropical cyclone forecasts are inaccurate. A 24-hour forecast tells us the precise latitude, and longitude where the cyclone will be located 24 hours hence, and it tells us what the maximum wind speed will be and how far 50 and 30 kt winds will extend outward from the center. The problem is that we can only be sure it won't happen that way, at least not quite. Typically the position will be off by 80 n mi, the wind speed by 10 kts and the radius of 50 and 30 kt winds will be off by 50%. We recognize that there is some threat of damage and personal injury at points in and near the forecast path of a tropical cyclone. We want to introduce the use of probability as a step toward quantifying this threat.

1.1.2 Decisions Based Upon Probability

Any time a rational person decides between alternative courses of action, he has estimated that, under probable outcome conditions, he will be better off with the selected choice than with any other.

A simple case, which occurs frequently in real life hurricane or typhoon evacuations is deciding whether to move a boat to an inland shelter or to leave it tied to an exposed pier. Let's make some estimates of the factors involved. The relevant factors are:

C = Cost of evacuation

L = Value of boat (potential loss)

V_c = Critical wind speed - the maximum wind which the boat can withstand (stronger winds will destroy it, weaker winds will do negligible damage).

We recommend moving the boat only if the moving cost is less than the probable loss if it is left, or

$$C < P(V_m > V_c) \cdot L \quad .$$

Where

$$P(V_m > V_c)$$

is the probability that the observed maximum wind (V_m) is greater than the critical wind. This expression is usually rearranged and read: Act only if $P(V_m > V_c) > C/L$.

For example, suppose it costs $100 to move a $10,000 boat to safety and our critical wind speed is 50 kts. Then C/L = .01 = 1%, thus we would move the boat only when the probability of 50 kt winds (or greater) exceeds 1%.

This is a workable relationship despite the difficulty in estimating C, L and V_c. The typical case is that potential losses are so much greater than preparation costs, that the "action probabilities" are typically very small and very crude estimates of C, L, and V_c don't greatly change the outcome.

There is a common sense precaution associated with this rule which can be illustrated by our boat moving example. When we arrived at 1% as the "action probability" of 50 kt winds we note that if the probability is 1 or 2% (either of which qualify) the probability of the maximum wind being less than 50 kts is 98 or 99%. If it takes

only a few hours to move the boat, we should wait until we can just comfortably complete the move before the onset of inclement weather. Thus we don't waste our effort and we give nature as much opportunity as possible to get us off the hook. The reaching of the "action probability" then is a necessary but not a sufficient condition.

The above extends easily to choosing between three alternate courses of action. Consider the following example of a medium sized, and hypothetical, police force which will man various emergency posts dependent upon which of 3 hurricane events is forecast. We assume the most likely (the mode) will be forecast.

Minor event requires 2 man days
Moderate event requires 10 man days
Major event requires 50 man days

There are "penalty" costs associated with either underestimating or overestimating the requirements which are expressed in man days in the following cost table. The elements on the diagonal represent the cost of correct manning, and those off the diagonal represent the cost of either over- or undermanning.

		Actual Occurrence		
	Action Options	Minor	Moderate	Major
1	Man for minor event	2	17	97
2	Man for moderate event	11	10	85
3	Man for major event	60	55	50

Cost contingency table for hurricane manning (man days)

A rational decision is one which minimizes the expected cost. If we can estimate the probabilities of each outcome occurring P_1, P_2, P_3, then the expected cost if we use:

Option 1 is $C_1 = 2xP_1 + 17xP_2 + 97xP_3$,

Option 2 is $C_2 = 11xP_1 + 10xP_2 + 85xP_3$, and

Option 3 is $C_3 = 60xP_1 + 55xP_2 + 50P_3$.

For example suppose $P_1 = .45$, $P_2 = .35$ and $P_3 = .20$. Note that we assume no other outcome is possible (minor includes no event) $P_1+P_2+P_3 = 1.00$.

$C_1 = 2x.45 + 17x.35 + 97x.20 = 26.25$

$C_2 = 11x.45 + 10x.35 + 85x.20 = 25.45$

$C_3 = 60x.45 + 55x.35 + 50x.20 = 56.25$

Since C_2 is the course of action with the minimum expected cost, it should be selected. Notice that the minor event is the most probable, but in this case, the best bet is slight over preparation. The difference in C_1 and C_2 may be trivial, but certainly either is preferable to C_3.

Figure 1 summarizes this problem in three graphical depictions. Figure 1a shows a 1x1 graph of P_1 vs P_2. Note for any P_1, P_2, a value of P_3 is determined since $P_3 = 1.0-P_1-P_2$. Thus in the lower left corner P_1 and P_2 are small, and P_3 is near 1. The space blocked off in

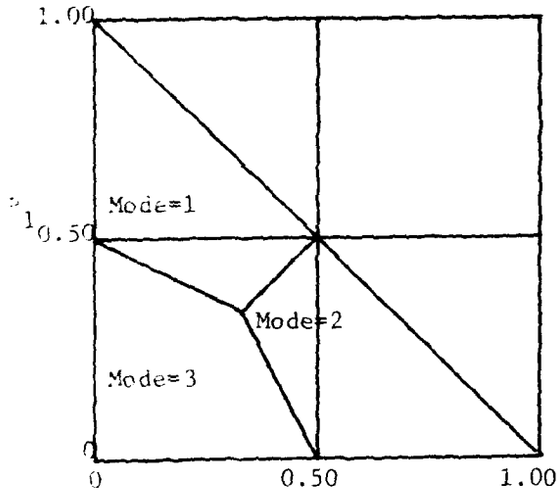

Figure 1a. Illustrates sections of a 1x1 probability square wherein events 1, 2 or 3 are the most likely of the three mutually exclusive events which are also exhaustive ($P_1+P_2+P_3 = 1.0$)

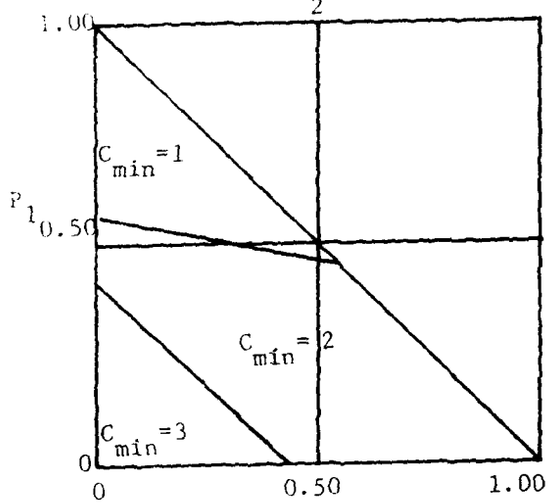

Figure 1b. Illustrates sections of a 1x1 probability square wherein the expected cost is minimized by planning for events 1, 2 or 3.

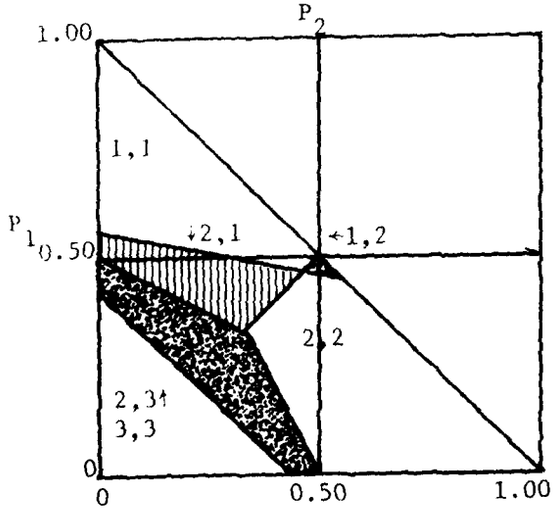

Figure 1c. Combines figures 1a and b. Illustrates conditions under which over-preparation (vertical hatching) and underpreparation (black) minimizes expected cost. Number pairs (N_1, N_2) are minimum expected cost event, most likely event.

the lower left is the region where event 3 (major hurricane event) is more likely than either events 1 or 2. Similarly the upper left and lower right represent the combinations wherein events 1 and 2 respectively are the most likely outcome. Notice that combinations of P_1, P_2 in the upper right triangle do not exist since $P_1+P_2 \leq 1$.

Figure 1b is a graphical representation of all possible combinations of P_1, P_2 and the minimum expected cost of each for the police department problem. Note there is a similarity between figures 1a and b. Near the corners where the outcome is fairly certain, the most likely outcome is the best one to plan on; however, in the middle region that is not true.

Figure 1c combines figures 1a and 1b. In the area with vertical cross-hatching, the most likely event to occur is one, a minor event; however,the expected cost is less in this region if we provide more manpower than that which is most likely required. In the shaded regions, the least expected cost occurs when we underman.

This type argument can be extended to any number of possible courses of action, although the computations become laborious. Graphical solution is restricted to 3 or less. A programmable calculator could nicely handle up to 5 or 6 options.

It should be noted that a categorical forecast does not provide the information required for this type of risk analysis. The difficult part of applying these methods is obtaining the probabilities. Providing the probabilities is the subject matter of this research.

1.2 Basis for Wind Probability

When a large supertyphoon is only a few hours away from us and closing, we can make a pretty fair estimate of the probability of 30 or 50 kt winds occurring at our position. When the same supertyphoon is several days away and/or forecast to pass some distance away we have great difficulty in making such an estimate.

In the following discussion we will illustrate the factors involved in wind probability estimates. These are the same factors we have always considered in tropical cyclone evasion planning, but we are now consolidating their effect into a single number. For purposes of illustration we will refer only to the probability of at least 50 kt winds. Similar development could be made for 30 kt winds.

Figure 2 illustrates a simple 24 hour tropical cyclone forecast. The hurricane symbol on the right is the nowcast position surrounded by a circle representing the radius of 50 kt winds. The dashed circle represents the same information for a day later. The latter is a forecast and as such is subject to error. The "x" in figure 2 represents the point of interest which might be an island or our ship's intended position. If our point is located within the 50 kt wind radius, it will experience winds of at least 50 kts. The factors involved are d, the distance from the cyclone to our point and R_{50}, the radius of 50 kt winds.

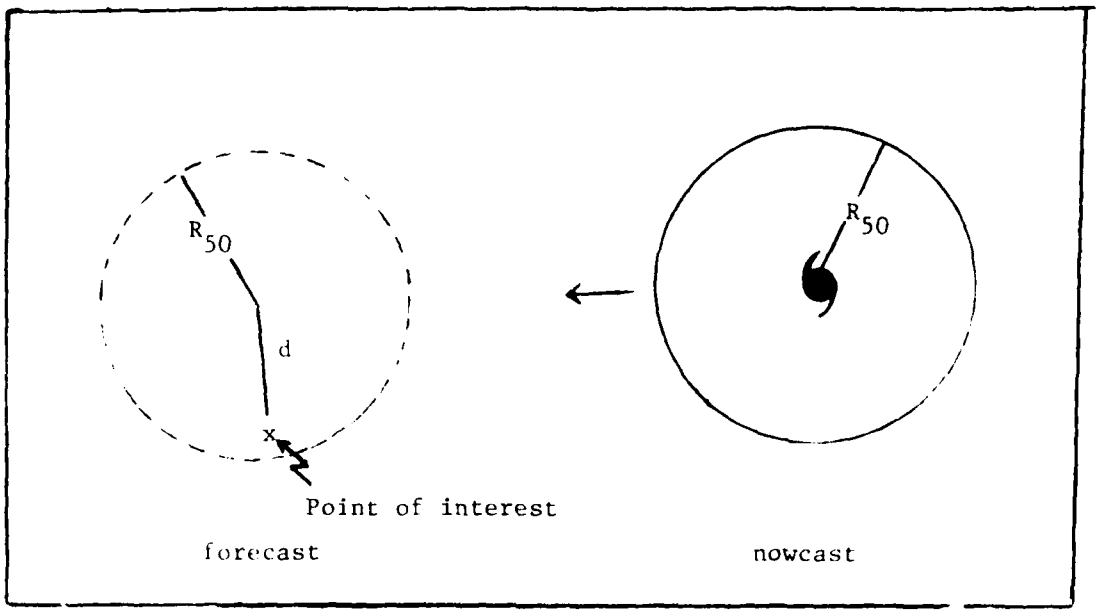

Figure 2. Schematic of typhoon forecast. Typhoon is forecast to pass point of interest so that point will be within 50 kt isotach.

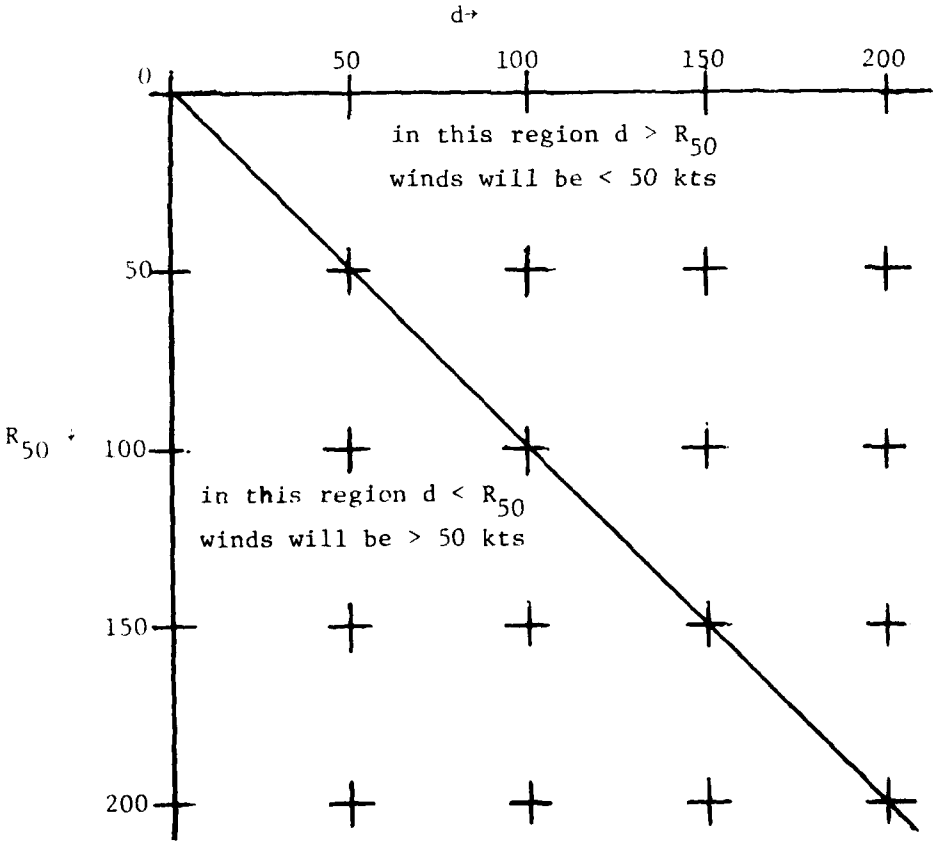

Figure 3. Schematic of possible relation of passing distance (d) to the radius of the 50 kt isotach (R_{50}).

Figure 3 relates d and R_{50}. Notice that anytime d is less than R_{50}, our point is inside the 50 kt wind circle and will receive winds over 50 kts. The lower left of figure 3, represents the "hit" region. any combination of d and R_{50} in the "hit" region gives rise to 50 kt winds at our point.

Both d and R_{50} are available from the forecast. R_{50} is given directly and d can be computed or measured. What we really would like to know is the verifying d and R_{50} since we know these will differ from the forecast. We, of course, won't have the verifying values until after the fact but we can estimate the probability of all possible values occurring.

A forecast error making the cyclone's closest point of approach (CPA) nearer to our point or making the radius of 50 kt winds larger than anticipated increases the threat of 50 kt winds. The opposite is also true in that combinations of an increase in CPA distance and a decrease in R_{50} greatly reduce the threat. An increase in both or decrease in both tend to be offsetting and hence may alter the threat little.

Figure 4 presents a depiction of these probabilities for a hypothetical 115 kt typhoon which is forecast to pass 100 miles from our point with a 50 kt wind radius of 90 n mi.

Figure 4a shows a 24-hour histogram of R_{50} for the case typhoon 25 nmi increments which is based on a study of maximum wind and wind radius forecast errors. The distribution is somewhat skewed to the left because the 0-25

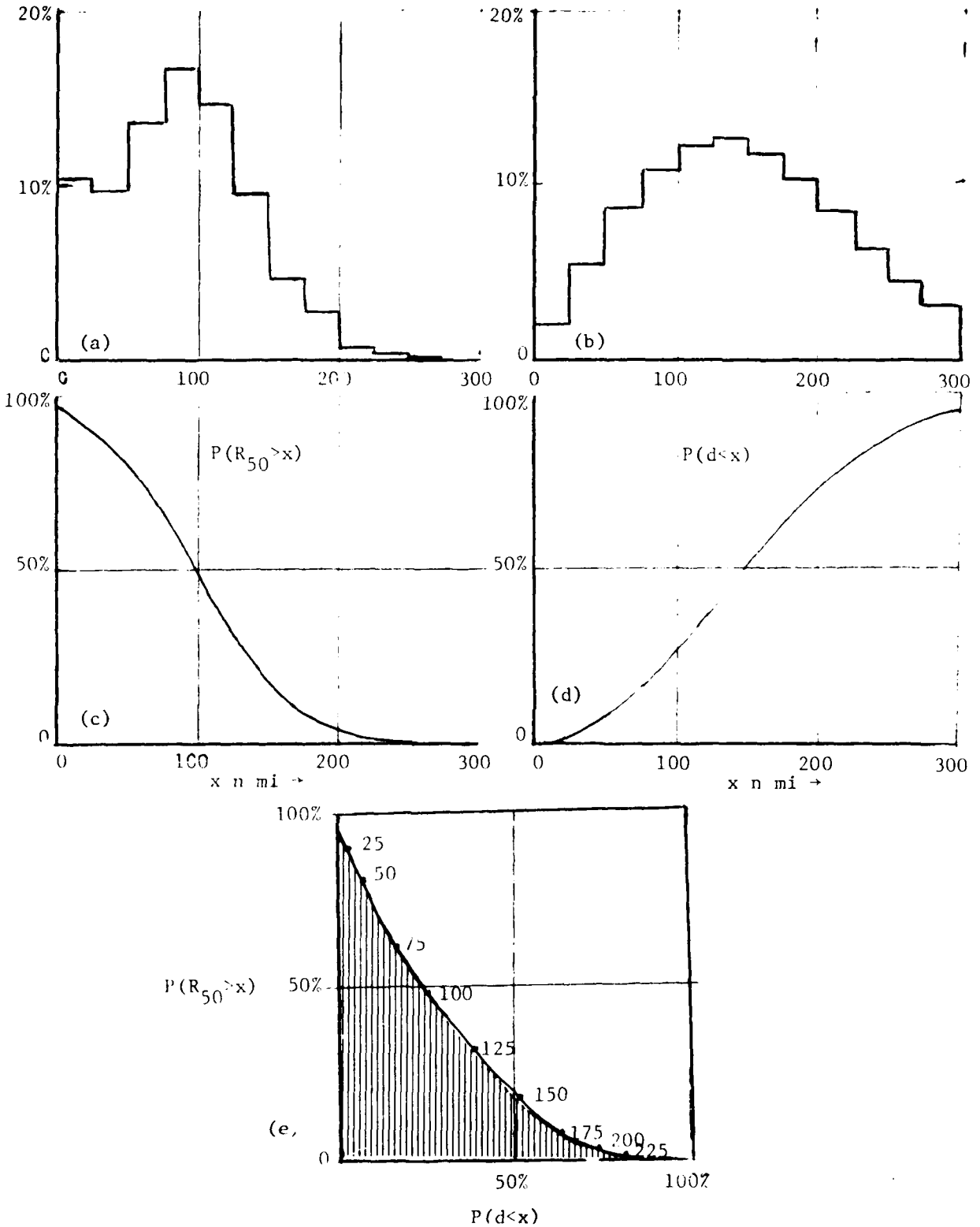

Figure 4. Depiction of probability density distribution of the radius of 50 kt isotach, R_{50} (4a), passing distance, d (4b), 4a summed right to left (4c), 4b summed left to right (4d), and 4e is a combination of 4c and 4d.

nmi grouping includes all the cases where the maximum wind is less than 50 kts.

Figure 4b shows the probabilities of the case cyclone passing within various distances of our point of interest in 25 n mi increments. These are computed by the STRIKP program. Figure 4c is a summation from right to left of figure 4a so that the probability that R_{50} is greater than x is depicted.

Figure 4d is a summation from left to right of figure 4b so that it depicts the probability that d is less than x. These two curves are then combined in figure 4e where coordinates are probabilities. This square graph can be thought of as all possible outcomes, where the lower left (cross hatched) section represents all possible cases where $d < R_{50}$. This is the requirement for observing 50 kt winds at our point of interest. The cross-hatched area is 29% of the total, inferring that the probability of our point receiving 50 kt winds is 29%.

1.3 User Information

The WINDP concept is a model, and as such it is based on a series of assumptions which generally apply but under certain conditions may be invalid. The following is intended to give the user insight into the model assumptions so that he can recognize situations where the assumptions and hence the results are suspect.

1.3.1 Forms of Probabilities

Probabilities are rounded to nearest whole percent. They are provided relative to 3 events occurring at 7 different times or within 7 different time periods after the forecast time.

The events are:

Strike will occur: The typhoon center will pass through an area defined by the user.

50 kt winds: Sustained winds of at least 50 kts will be observed at the point of interest.

30 kt winds: Sustained winds of at least 30 kts will be observed at the point of interest.

The times are 0, 12, 24, 36, 48, 60 and 72 hours after the warning time. Probabilities are given in two modes, instantaneous and time integrated. For example, the 24 hour instantaneous event means that the occurrence would be observed at 24 hours after forecast time (forecast initial time). The corresponding time integrated event means that the occurrence would be observed within that 24 hour period (0-24 hours after forecast time). While the capability exists to time integrate the probability over any time interval it is only published for time

intervals beginning at 0. The probability for an included interval cannot actually be inferred from the published information but might be estimated as follows:

If $PS_{t_1t_2}$ is the time integrated probability over the time interval (t_1,t_2) and, PI_{t_1} is the instantaneous probability at time t_1 then $PS_{t_1t_2}$ can be approximated by

$$PS_{t_1t_2} \doteq PI_{t_1} + (PS_{0t_2} - PS_{0t_1}) , \quad \text{where}$$

this will be an underestimate of $PS_{t_1t_2}$. The error will be negligible for small PS_{0t_1} (<5%) increasing to the point where it is not recommended for $PS_{0t_1} \geq 50\%$.

1.3.2 Accuracy of Probabilities

Since we have defined probability as an estimate to a quantity that really cannot be measured, the term accuracy has little meaning here. We never show more than two significant numbers. This is partly due to the need to compact data for message transmission, but the important reason is that the additional precision afforded by an additional digit is nonsense. Testing indicates the numbers are roughly valid to within 10% of their value (see section 2.7); that is a probability of 10% should be regarded as 9-11%. The accuracy of small probabilities (below 10%) is limited by the number of significant digits given; therefore 1% should be regarded as being within the range 0.5% to 1.5%. This is considered to fairly reflect the actual precision in the number and not to warrant reporting to more significant digits. For this reason we never consider a predicted probability to be precisely 0 or 1. Hence we use the symbol

(IN-insignificant) instead of those values (<0.005) which would round to less than 1%, and at the other end we artifically constrain probabilities to ≤99%.

1.3.3 Input Errors

By far the most common problem with WINDP or STRIKP is erroneous input data. There is an internal check on the input track forecast. Any motion which is unusual (would be expected to occur only 5% of the time naturally) is flagged. When this flag "UNUSUAL MOTION NOTED ALONG FORECAST TRACK" is received, the input forecast should be compared with the warning center message for accuracy. In the event of discrepancies, FNOC should be notified, but the output should be viewed as suspect. The same advice applies to discrepancies in wind speeds also.

1.3.4 Land Influences

Wind probabilities are doubtful over land. This is true because wind forecasts reflect track forecasts with respect to landfall and length of the forecast overland stay. To the extent the track forecast with respect to land is inaccurate, the wind forecast will be biased. This bias should be minor for islands and for coastal areas when the cyclone is approaching from seaward. Land influences are manifest as rapid decreases in the instantaneous wind probabilities, most notably the 50 kt wind probability, near forecast landfall time. If the point of interest is inland, probabilities will be too large. For the case where the point of interest is coastal or in open water and the forecast is overland, probabilities will be understated. In both cases the time integrated probabilities will be less biased than the instantaneous probabilities.

1.4 Input/Output

1.4.1 The input for the WINDP model is by card image and includes only information sufficient to identify the proper tropical cyclone in the FNOC files and a geographical position about which the threat is to be evaluated. This latter information is stored internally for 9 Western Pacific points and will be retrieved if no geographical coordinates are provided. As a matter of convenience the STRIKP program is built into the WINDP program so radii to the right and left (relative to forecast track) of the point of interest are required to define the "strike" area.

The following information is required input:

- Cyclone name, i.e., WANDA, TD02, TC17-80
- Ocean Basin - NA (North Atlantic), EP (Eastern Pacific), WP (Western Pacific) (WINDP is presently valid for the Western Pacific only)
- Cyclone number - consecutive basin number for year
- Month, Day and GMT Hour of forecast
- Number of tropical cyclones in basin (West-Pac only)*
- Latitude/Longitude of point of interest*
- Radius left and right (relative to forecast track)* which defines strike area

*Values will be calculated or assigned if not provided.

1.4.2 Output

The WINDP output is presented in three modes: (1) Individual users mode (2) standard nine point mode and (3) field data for Naval Environmental Display Station (NEDS).

1.4.2.1 Individual User Request: This output is illustrated in figure 5. Featured are strike, 50 kt wind and 30 kt wind probabilities at 12 hour intervals to 72 hours after forecast issue time. Instantaneous and time integrated probabilities are provided. Additionally, the forecast which forms the basis for the probability estimates is given in abbreviated form for validity checking.

1.4.2.2 Standard Nine Point Output: This output is illustrated in figure 6. The format is similar to that of figure 5. A forecast difficulty class is provided for JTWC (See Jarrell, et al, 1978).

1.4.2.3 Field Data Output: This output is derived by inputting the latitude/longitude of FNOC global band grid points as the point of interest in the WINDP model. Of the 42 values computed at each grid point (strike, 50 kt and 30 kt, instantaneous and time integrated, at 7 time steps 0 - 72 by 12 hours (3x2x7)), 18 of these are retained. These are strike, 50 and 30 kt, instantaneous and time integrated at 24, 48 and 72 hours (3x2x3=18). Samples are shown in figures 7 and 8.

Figure 7 (top) illustrates a forecast for typhoon OWEN in September 1979. The bottom portion of the figure illustrates contours of the instantaneous probability of 50 knot (or greater) winds from OWEN at 24 hours, 48 hours and 72 hours (left to right). Notice that instantaneous probabilities tend to decrease with time. This is because as uncertainity increases (farther into future), the threat to any point near the forecast track decreases as those far from the track increase. Note the spreading of the 2% contour and simultaneous contraction of the 10% contour from 24 to 48 hours. The total probability that 50 kt winds

```
STRIKE AND WIND PROBABILITY FORECASTS FOR TROPICAL CYCLONE OWEN

FROM 260600Z BASED ON FOLLOWING FORECAST
002371290100 122481286105 242601285110 482871311085 723121363065
STRIKE IS BEING WITHIN 50NM RIGHT AND 75NM LEFT OF 26.3N 127.7E

STRIKE PROBS 00ININ 121115 242431 360832 480332 600132 720132
50 KT WINDP  000505 124041 244649 361950 480750 600250 72IN50
30 KT WINDP  005151 128282 248183 365983 483183 601183 720383
```

Figure 5. Example of output in response to an individual user request. The "user" identified Typhoon OWEN, warning at 260600Z Sept 1979 and specified area of interest as 75 n mi left and 50 n mi right of 26.3°N 127.7°E.

```
STRIKE AND WIND PROBABILITY FORECASTS
OWEN     260600Z
SUBIC BAY THREAT NIL
CLARK AB  00ININ 12ININ 24ININ 36ININ 48ININ 60ININ 72ININ
  50 KNOT 00ININ 12ININ 24ININ 36ININ 48ININ 60ININ 72ININ
  30 KNOT 00ININ 12ININ 24ININ 36ININ 48IN01 60IN01 72IN01
APRA GUAM THREAT NIL
ANDERSEN  THREAT NIL
KADENA AB 00ININ 121115 242431 360832 480332 600132 720132
  50 KNOT 000505 124041 244649 361950 480750 600250 72IN50
  30 KNOT 005151 128282 248183 365983 483183 601183 720383
YOKOSUKA  00ININ 12ININ 24ININ 36ININ 48ININ 600101 720105
  50 KNOT 00ININ 12ININ 24ININ 36ININ 48ININ 600102 720106
  30 KNOT 00ININ 12ININ 24ININ 360101 480307 600713 720616
KEELUNG   00ININ 12ININ 24ININ 36ININ 48IN01 60IN01 72IN01
  50 KNOT 00ININ 12ININ 24ININ 36IN02 48IN03 60IN04 72IN04
  30 KNOT 000707 121727 242028 361129 480530 600230 72IN30
YOKOTA AB 00ININ 12ININ 24ININ 36ININ 48ININ 600101 720105
  50 KNOT 00ININ 12ININ 24ININ 36ININ 48ININ 600102 720106
  30 KNOT 00ININ 12ININ 24ININ 36IN01 480307 600612 720616
HONG KONG 00ININ 12ININ 24ININ 36ININ 48ININ 60ININ 72ININ
  50 KNOT 00ININ 12ININ 24ININ 36ININ 48ININ 60ININ 72ININ
  30 KNOT 00ININ 12ININ 24ININ 36ININ 48ININ 60ININ 72IN01
FOR JTWC..CLASS= ONE
PROBABILITIES BASED ON FOLLOWING FORECAST
002371290100 122481286105 242601285110 482871311085 723121363065
```

Figure 6. Example of standard output for 9 preselected western Pacific points. The strike areas are within 75 n mi left and 50 n mi right of these points.

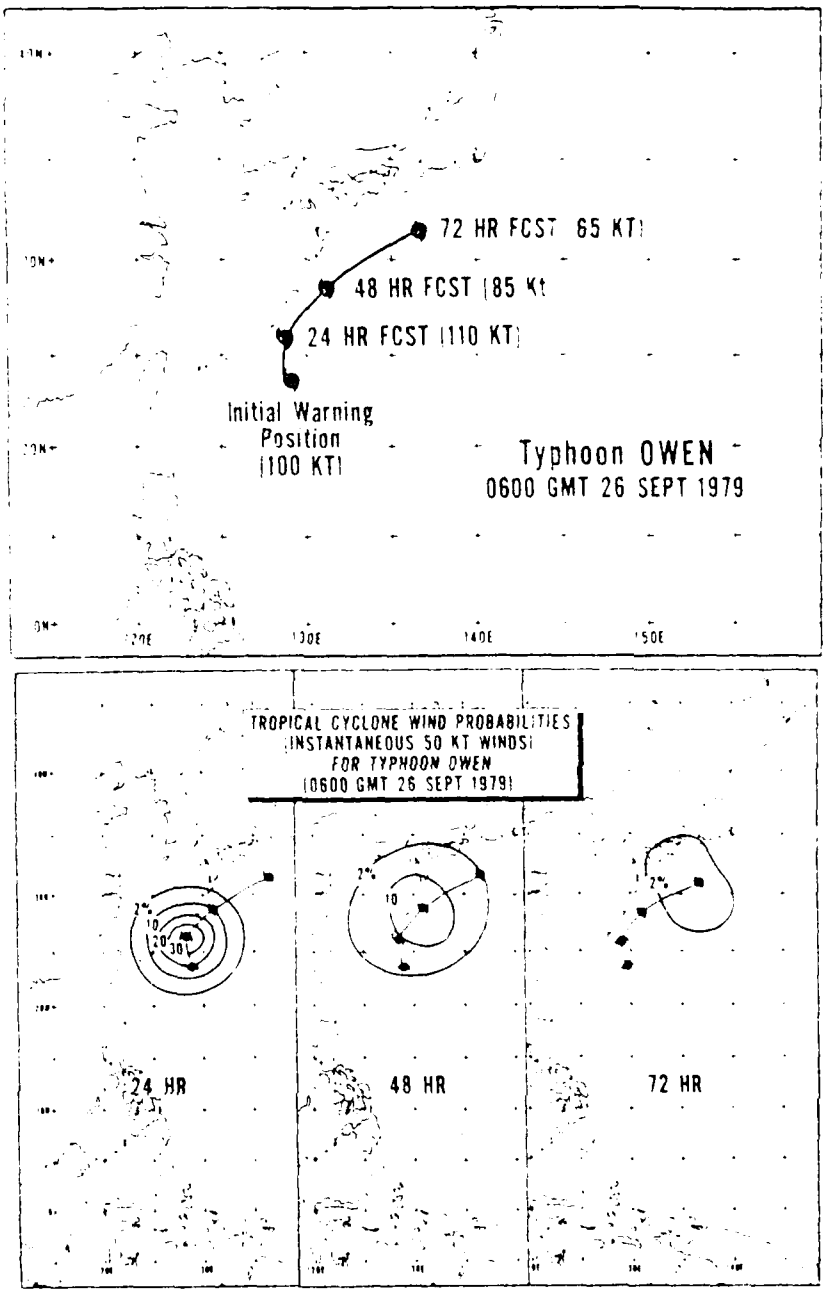

Figure 7. Top: Plot of a forecast of typhoon from 0600 GMT 26 September 1979.
Bottom: Map of the instantaneous probabilities of 50 kt winds occurring 24, 48 and 72 hours later.

or greater will be observed at any point decreases in this case because the maximum wind is forecast to decrease after 24 hours from 110 kts down to 65 kts. While there is little probability of maximum winds not exceeding 50 kts at 24 hours (when 110 kts is forecast), there is a substantial probability (about 42%) that the 72 hour maximum, which is forecast to be 65 kts, will be in fact less than 50 kts.

Figure 8 is another example of the NEDS type output. This is a representation of some of the time integrated probabilities for supertyphoon Hope as she was beginning to threaten Hong Kong in late July 1979. Figure 8a depicts the forecast. Hope was expected to pass through the Luzon Straits and make landfall on China in less than 48 hours. The maximum wind forecasts are strongly dominated by the track forecast, since in the absence of landfall, the 48 hour forecast would almost certainly have been over 100 kts vice the 35 kts actually forecast. *Figure 8b illustrates the 24 hour time* integrated probabilities for strike, as well as 50 and 30 kt winds. Figure 8c depicts the same probabilities within 48 hours. Note that the 50 kt wind probabilities are larger than the strike probabilities and smaller than the 30 kt wind probabilities. The latter is, of course, always true but the former is true only if the expected radius of 50 kt winds is greater than the radius of the "strike" area.

Notice that in comparing the 48 hour plot to the 24 hour plot, the time integrated probabilities increase (or remain constant) in time. The point of maximum probability is displaced slightly ahead of the initial point. While the maximum probabilities for a typhoon will usually be near 100% at the initial point, this will rarely be truly

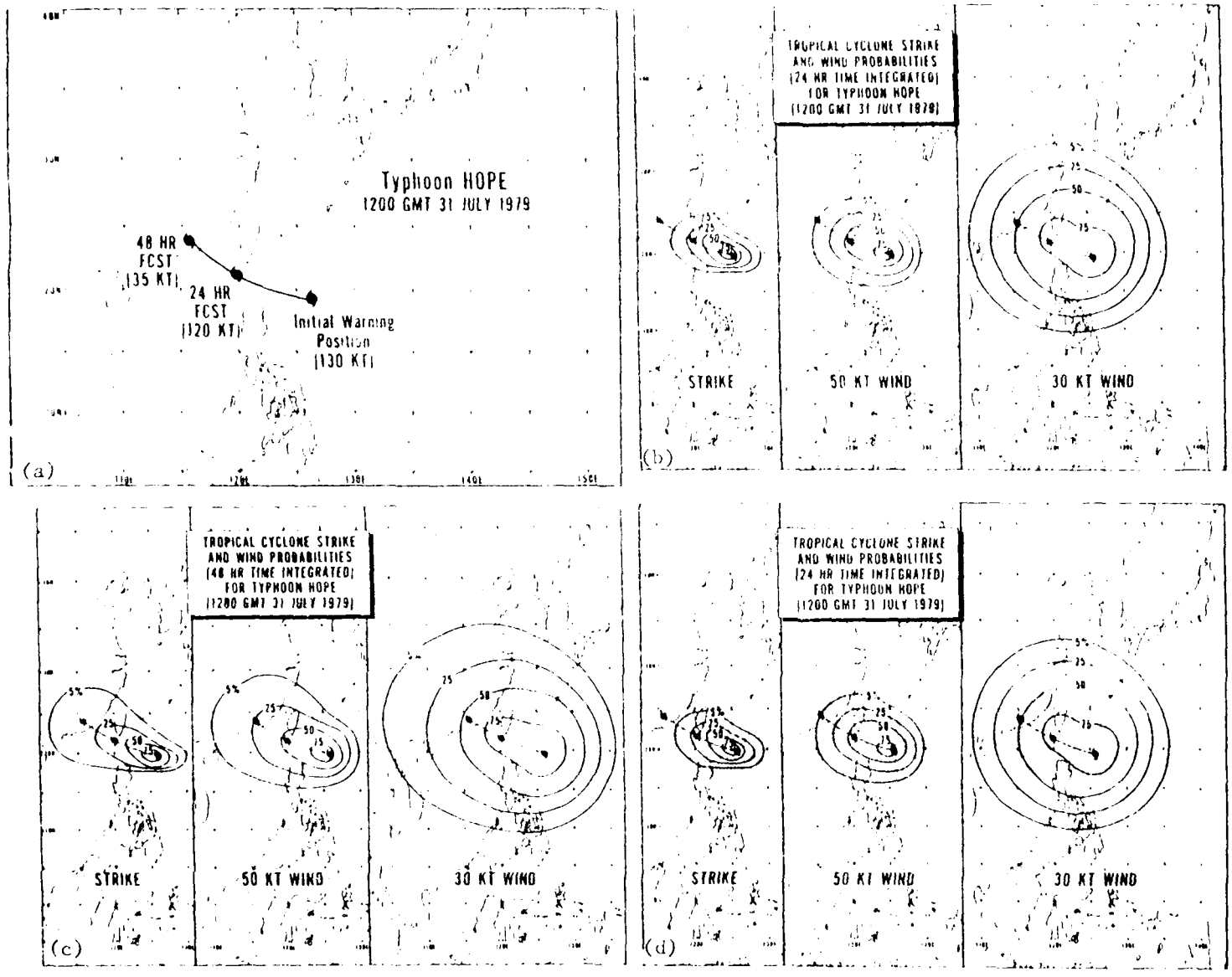

Figure 8. (a) Plot of a forecast of typhoon HOPE from 1200 GMT 31 July 1979.
(b) Maps of probability of strike (see text for definition), 50 kt and 30 kt winds at any time within 24 hours.
(c) Same as (b) only within 48 hours.
(d) Same as (b) except CINCPACFLT danger area is superimposed on maps.

represented on the plot because of the coarseness of the grid unless the initial point nearly coincides with a grid point. This deficiency is considered to be of no importance since high probabilities are expected there. The grid spacing is quite adequate to represent the distribution of probability away from the center.

In figure 8d, the 24 hour strike and 50 and 30 knot wind probability plots have been overlaid with a danger area plot as defined by Commander-in-Chief, U.S. Pacific Fleet. This suggests some inconsistencies in levels of safety inherent in using this type of plot. First notice that the danger area equates to a 30 kt wind threat of about 40% ahead of the typhoon and about 60% behind the typhoon. Whether this difference is justifiable on the basis that greater risk is acceptable behind than ahead of the cyclone is unlikely. Notice that the danger area in this case closely coincides with the 5%, 50 knot wind probability. It should be noted that for larger (smaller) cyclones this 5% contour would be larger (smaller) as would the CINCPACFLT danger area, and both would also increase in size with increasing forward speed. Unlike the CINCPACFLT danger area, however, the 5% contour would also vary as a function of forecast difficulty, allowing more safety margin for more difficult forecasts. Some easily described variation on the 5% 50 kt WINDP contour might be developed which would more consistently provide the safety margin that CINCPACFLT desires.

Section 2

TECHNICAL SECTION

2.1 Introduction

The intent of this section is to provide information useful to anyone involved in either extending or modifying this work. This represents the scientific documentation of the models theoretical basis, assumptions and supporting documentation as well as a sample model calculation and the results of some independent data testing.

2.2 Theoretical Basis for Wind Probability

We assume that in a tropical cyclone winds measure from a background value of V_o at distance from the center r_o toward the center of the cyclone to a maximum (V_m) at a radius (R_m) from the center. Then it follows that, an isotach of a wind speed of concern ($V_o<V_c<V_m$) exists at some distance ($R_m<R_c<r_o$). With this basis we assert that if the cyclone passes at distance (D) from a point of interest, that point will at some time observe winds in excess of V_c if, and only if, $D<R_c$.

The probability of this occurring is given by $P(D<R_c)$. In the strike probability model this is determined by integrating a bivariate normal probability density function over a circle of radius R_c centered on the point of interest. Notice that any position (and hence a distance D between two positions) can be expressed as a forecast position (lat, lon) and a forecast position error. The bivariate normal function follows an assumption that forecast position errors are so distributed about the

forecast position. The WINDP model takes this one step further and assumes that R_c is also a random variable. Now the probability of observing winds of V_c is given by the joint probability: $P(D<r, R_c=r)$ or $P(D=r, R_c>r)$ summed over all possible values of r.

It is important to note that the foregoing assumes that the maximum wind is at least as great as V_c. Therefore the more general probability expression is $P(D<r, R_c \geq r, V_m>V_c)$.

We have some information about the relationship between D, R_c, and V_m. To a reasonable approximation, we can approximate R_c from R_m, V_c and V_m using the Riehl (1963) profile $Vr^{0.5}$ = const, or $R_c=(V_m/V_c)^2 R_m$. Using the JTWC warning data and inferring R_m from the radius of 50 kt winds or the radius of 30 kt winds and V_m, we note a rather strong linear relationship between R_m and V_m (ρ = -.64). This is expected since the relationship for R_m involves V_m^{-2} (inverted from above). The occurrence of a particular combination of D and V_m can be expressed as a particular deviation from a forecast state (position and maximum wind). An examination of a sample of forecast errors, rather surprisingly, suggests these deviations are independent. (See section 2.3.1.3). Based on small correlations between position error components and maximum wind forecast errors and the known relationship between maximum wind and radius of maximum wind, errors in the forecast of position are assumed to be independent of errors in the forecast of the wind profile (maximum wind and radius of maximum wind). Hence the joint probability:

$$P(D<r,\ R_{c-}\geq r,\ V_m>V_c) = P(D<r)\cdot P(R_{c-}\geq r,\ V_m>V_c) \ .$$

The last term on the right can be written:

$$P(R_{c-}\geq r,\ V_m>V_c) = \sum_{V_i=V_c}^{V_i=\infty} P(R_{c-}\geq r,\ V_m = V_i) \ ,$$

or equivalently:

$$= \sum_{V_i=V_c}^{V_i=\infty} P(R_{c-}\geq r \mid V_m=V_i)\cdot P(V_m=V_i)$$

The probability then that a point will receive winds of at least V_c is estimated by summing this over all r values

$$\sum_{r_j=0}^{r_j=\infty} P(D=r_j) \qquad \sum_{V_i=V_c}^{V_i=\infty} P(V_m=V_i)\cdot P(R_{c-}\geq r_j \mid V_m=V_i) \ .$$

Term 1 Term 2 Term 3

2.2.1 Computation of Probability Terms

Term 1 is computed just as in the STRIKE probability model. The spatial integration of the bivariate normal probability function is performed over a narrow ring centered about the point of interest with mean radius r_j.

Terms 2 and 3 are based on multiple linear regression equations which predict R_m and V_m as a function of several predictors, but most importantly, the forecast of R_m (implied from R_{30} and R_{50}) and V_m issued by the JTWC. In the development of the regression equations for R_m, "perfect" information on V_m was used as a predictor. This is necessary because the form $P(R_c \geq r | V_m = V_i)$ assumes a known V_m. (See Sec. 2.2).

Term 2 uses a multiple linear regression equation for the maximum wind in the form $V^* = a_o + a_i X_i \ldots a_n X_n$, where the X_is are the predictors. The probability $P(V_m = V_i)$ is calculated by assuming that the actual maximum is normally distributed about a mean of V^* with a standard deviation equal to the standard error of the regression equation. (See section 2.3.1.2.) This normal function is then integrated over a small interval centered on V_i.

Term 3 uses V_i above among other parameters in a regression equation for the radius of maximum winds R^* in the form

$$R^* = b_1 + b_1 X_1 + \ldots + b_n X_n.$$

The actual verifying R_m is assumed to be normally distributed about a mean of R^* with a standard deviation equal to the standard error of the regression equation. A value of R_{ij}, the radius of maximum wind which would be required with maximum wind V_i to produce a radius of the V_c isotach equal to r_j is given by

$$R_{ij} = r_j (V_c / V_i)^2 .$$

The probability,

$$P(R_{c} \geq r_{j} | V_{m}=V_{i})$$

is then equated to $P(R_{m} \geq R_{ij})$ and obtained by integrating the assumed normal function from R_{ij} to infinity.

2.3 Wind Error Study

Data: Two data sets were used in this study. The first set was assembled at NEPRF (Brody, et al, 1979). It includes information relative to the nowcast (0 hour forecast) from the Joint Typhoon Warning Center (JTWC) tropical cyclone warnings.

Included is:

- Date time information
- Storm identifying number
- Position (latitude and longitude)
- Maximum wind (this is post analysis, as opposed to nowcast information) in knots
- Radii information for 100-, 50-, and 30-kt winds (i.e., when maximum winds exceeded these values) in n mi

The data set covered the years 1966-77, however only the 6 years 1972-77 were used in this study. It should be noted that this set does not include tropical depressions.

The second data set was reduced by SAI from JTWC warnings held by Fleet Numerical Oceanography

Center, NEPRF or the Naval Postgraduate School. This accounts for roughly 80% of the warnings issued by JTWC during the 1972-77 time period.

This set includes:

- Storm identifying number
- Forecasts at 12-, 24-, 48- and 72-hours of:
  - Latitude and Longitude
  - Maximum wind (in knots)
  - Radius of 50 kt winds (n mi)
- Forecasts of radius of 30 kt winds at 24 hours.

The two sets were matched so that essentially all the information from JTWC forecasts was on one record. During this time JTWC issued 3374 warnings, with about 60% of them appearing complete in this file. Part of the missing data is attributable to the exclusion in the NEPRF file of warnings during the tropical depression stage and another part is due to missing warnings in the SAI set. The latter consist mostly of occasional missing records within a cyclone which are of little consequence since a single warning offers virtually no independent information above that contained in the adjacent warnings.

One further limitation was placed on the data set in that land influences were removed whenever possible. Using a FNOC sea/land routine, any forecast or verifying position near land and subsequent forecasts of the same warning were flagged for exclusion. "Near land" was determined by examining the position and 6 surrounding points equally spaced on a 60 n mi radius. If any two adjacent points of these seven were overland the position was flagged.

The NEPRF information was treated as ground truth for the purpose of forecast verification even though this was recognized as having limitations.

Radius information proved somewhat inconsistent. For example, 50 kt wind radius information is given in the 12-, 24-, 48- and 72-hour forecasts, while 100 kt radii information is given only in the initial forecast (nowcast), and 30 kt information is present only in the nowcast and 24 hour forecasts. When the wind is (or forecast to be) below 50 kts, no 50 kt radius information is given, thus no radius information would be available at 12-, 48- or 72-hours. To avoid losing this information some steps were taken to make the data consistent and to fill in for missing data. This is somewhat undesirable because a systematic model must be assumed. That assumption will thereafter impact the results, but without such a model we would be unable to handle cases with no forecast of 30 or 50 kt wind radii (low wind forecast).

To make everything consistent, all radii and max wind information was reduced to two numbers - maximum wind (V_m) and radius of maximum wind (R_m). This was done by using $Vr^{.5} = \text{const}$ (Riehl, 1963). With a maximum wind forecast (or observation), a radius of maximum wind could be inferred from the 30, 50 or 100 kt radius. The 100 kt radii data appeared to be inconsistent with the other information and was thus ignored. Where two usable estimates of R_m were possible (both 30 and 50 kt radii were given) a mean of the two was used.

To handle the cases where winds were forecast to be less than 50 kts in the 12-, 48- and 72-hour forecasts, a forecast radius of maximum winds was inferred from the 24-hour forecast by:

$$V_{mt}R_{mt}^{.5} = V_{m24}R_{m24}^{.5}$$

where t=12, 48- and 72-hours. For the few cases where the 24 hour radius was not usable, a simple regression equation was used (this was derived from the information in Table 2 section 2.3.1.2 below).

$$R_m = 73 - 0.46\ V_m \text{ in n mi.}$$

This would only occur with low winds. It should be noted that the intent here is to statistically handle the variations of the 50 and 30 knot wind radii from their forecasts (either explicit or implied). Any lack of ability in the Riehl profile to accurately specify the radius of maximum winds is academic since that pseudo radius is used only as a device to hold the 30 and 50 kt radii information. Attempts to extend the results of this study to high wind speeds (say 100 kts) would have to reckon with such a deficiency.

2.3.1 Statistical Results

The major findings of a statistical analysis of the maximum wind and wind radii study will be presented here. Several assumptions have been cited in the description of the WINDP model. Statistical support for those assumptions will be indicated among the information presented.

2.3.1.1 Forecast Verification: Anytime forecast errors are discussed, there is implied a knowledge of truth or verification data. For the verification of maximum wind forecasts, a post analysis of maximum winds by the JTWC serves as this truth. The truth basis for 50 and 30 kt isotach radii is far less solid. There is no post analysis, nor was one attempted in this study. Instead, the JTWC nowcast data was used as verification data. A further complication arises when we try to verify the implied radius of maximum wind since it is derived from the 30 and 50 knot isotach and the maximum wind. This is a mix of nowcast and postanalysis data, which can lead to some inconsistencies.

Table 1 presents a comparison of forecast and verifying maximum winds.

	Length of Forecast			
	12 hr	24 hr	48 hr	72 hr
Forecast maximum wind				
mean	69 kts	70 kts	72 kts	74 kts
standard deviation	26 kts	26 kts	25 kts	26 kts
Observed maximum wind				
mean	67 kts	67 kts	67 kts	62 kts
standard deviation	28 kts	31 kts	35 kts	38 kts
Correlation coefficients				
forecast to observed	0.84	0.76	0.60	0.47
initial to verifying	0.83	0.64	0.27	0.06
initial to forecast	0.92	0.84	0.66	0.48
Number of cases	1727	1338	1096	839

Table 1. Comparison of JTWC Forecasts to Observed Maximum Winds from Years 1972-77.

Table 1 reveals a rather pronounced bias toward overforecasting wind speed. The same tendency seems evident in the objective techniques used at the JTWC (JTWC, 1977), but not in their official verification (see, for example, JTWC, 1977). This apparent difference is probably related to our exclusion of land effect cases. The inclusion of these in the official verification would account for the over-forecasting by objective techniques since they are, without exception, designed for overwater use only.

The correlation between forecast and observed maximum winds is interesting when compared to the correlation between initial (nowcast) and the verifying winds 12, 24, 48 and 72 hours later (a measure of actual persistence) and between the initial maximum wind and the forecast (a measure of the forecaster perceived persistence). The implication here is that early forecasts are heavily persistence and, in fact, that maximum winds over the short term are highly persistent. One might conclude that the influence of persistence is too heavy on longer range forecasts; however it is clear that the forecaster, by whatever means clearly improves on persistence in long range forecasts (i.e., he has the right trend).

Brody et al (1979) compared the forecast change in the radius of 50 kt winds to the actual change. Figure 9 shows those results for the 24-hour forecast. He found that the correlation coefficients increased steadily from 0.45 in the 12 hour forecasts to 0.60 in the 72 hour forecast. The reason for the increase in time is again a reflection of the use of persistence in short range forecasts (constant change of zero is forecast) and the forecasters ability to specify the trend of the longer range change.

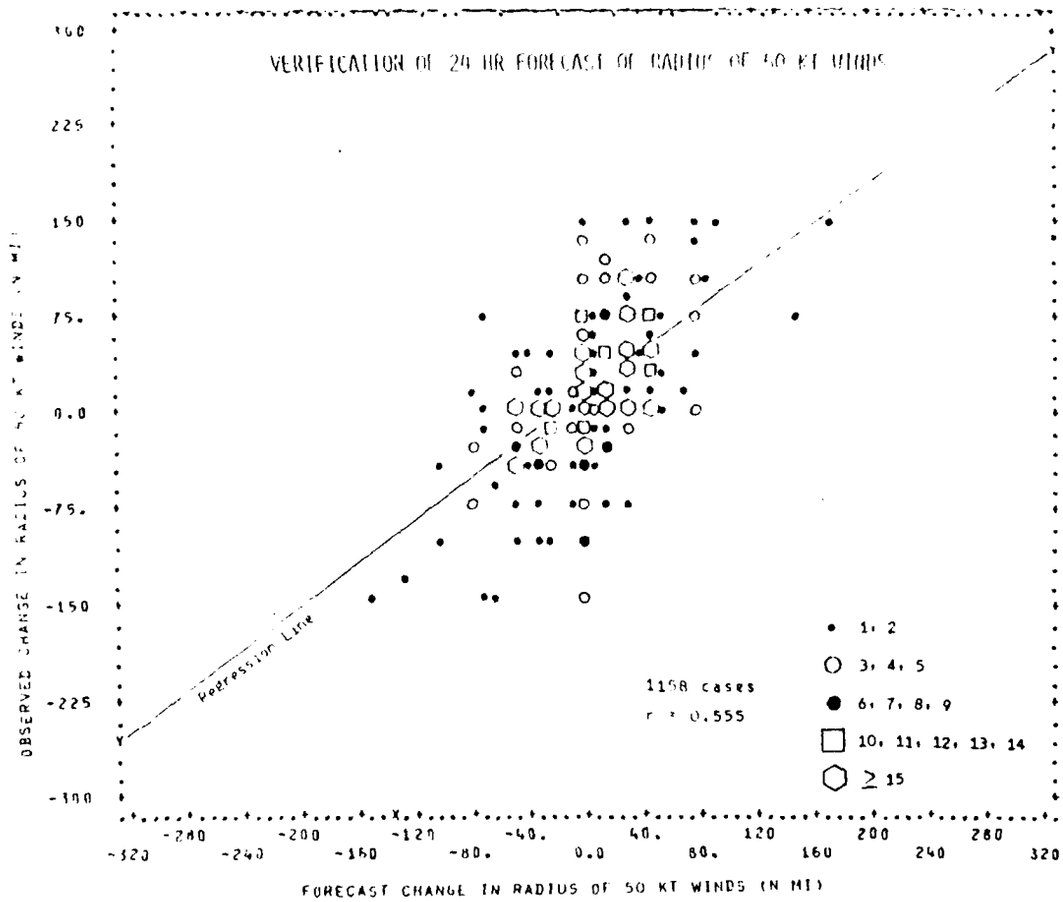

Figure 9. Comparison of 24 hour forecast to observed change in radius of 50 kt winds in typhoons. (Brody, et al, 1979)

Table 2 compares the implied radius of maximum winds, forecast to observed.

	Forecast Length			
	12 hrs	24 hrs	48 hrs	72 hrs
Forecast Max Wind Radius				
mean	38 nmi	37 nmi	34 nmi	33 nmi
standard deviation	18 nmi	17 nmi	17 nmi	16 nmi
Observed Max Wind Radius				
mean	39 nmi	38 nmi	37 nmi	38 nmi
standard deviation	18 nmi	18 nmi	18 nmi	18 nmi
Correlations				
observed to forecast	0.51	0.50	0.33	0.37
max wind to radius of max wind	-0.62	-0.65	-0.69	-0.72
Observed Max Wind				
mean	74.5	77.7	82.7	85.7
Number of cases	1399	1060	804	522

Table 2. Comparison of the Radius of Maximum Winds

It should be noted that the information required to compute radius of maximum wind is not available for verification when maximum winds are below 30 kts nor is the forecast information available when the maximum wind is forecast to be 30 kts or less. Thus the radius of maximum wind was not verified over the same range of cyclone intensities as maximum wind. Because of this, Table 2 differs from Table 1 in that it gives a smaller number of cases and larger mean observed wind speed.

The apparent under forecast in radius of maximum winds is a reflection of the same over forecast in maximum winds shown in Table 1, since the two are inversely related in the assumed profile. This is shown in the correlation between these two values in Table 2. The low correlation between the observed and forecast radius of maximum winds is not surprising and simply reflects the poor state of the measurement and understanding of areal wind distributions.

2.3.1.2. Regression Equations for R_m and V_m: Stepwise linear regression analysis was performed on both maximum winds and the radius of maximum winds. This was done to remove any systematic bias from the forecasts and also because the residuals from such an analysis provide a ready source of statistical information. Table 3 summarizes the results of that analysis.

	PREDICTANDS							
	Radius of Maximum Wind				Maximum Wind			
	12hr	24hr	48hr	72hr	12hr	24hr	48hr	72hr
PREDICTOR								
Verifying V_m	-0.62	-0.55	-0.50	-0.50	Predictand			
Verifying R_m	Predictand				Not allowed to enter			
Forecast V_m	Not allowed to enter				0.40	0.48	0.67	0.45
Forecast R_m	0.29	0.33	0.16	0.19	Not allowed to enter			
Forecast Lat	1.29	*	*	*	-0.45	*	*	*
Forecast Long	0.09	*	*	-0.43	*	-1.06	-0.24	-0.23
Initial Lat	-1.17	*	*	*	*	-0.50	-1.21	-1.88
Initial Long	*	0.09	0.14	0.58	*	0.96	*	*
Initial V_m	0.27	0.24	0.09	0.07	0.56	0.39	*	*
12hr chg V_m	*	*	*	*	0.42	0.49	0.41	0.50
12hr Speed	*	*	*	-0.57	-0.40	-0.85	-1.29	-0.74
INTERCEPT	39.1	39.3	47.7	49.0	12.3	36.8	84.3	97.5
r	0.72	0.72	0.73	0.76	0.89	0.83	0.69	0.59
r^2	0.52	0.52	0.53	0.58	0.79	0.68	0.48	0.35
STD ERR	12.	12.	12.	11.	13.	16.	25.	31.

Table 3. Results of stepwise linear regression analysis to predict radius of maximum winds (R_m) and maximum winds (V_m) at 12, 24, 48 and 72 hours. (*Not selected by stepwise screening.)

These regression equations are used to predict the maximum wind and the radius of maximum wind, and the residuals form the statistical basis for handling forecast errors. This is done by assuming the residuals to be normally distributed with $\mu = 0$ and σ = standard error.

Figure 10 are plots of the cumulative frequency distributions of the residuals from the regression equations of Table 3 on probability paper. The assumed normal distributions are shown as straight lines. With some minor exception agreement is very good. There is some insignificant disagreement in the tails, and the plot of the 12 hour forecast maximum wind residuals is significantly non normal at the 5% level using a Kolmogorov-Smirnov test. The observed distribution is too peaked. It is doubtful that this is serious in the present use.

2.3.1.3 Position Errors Related to Wind Forecast Errors:

A necessary and sufficient condition to cause winds of 50 kts to be observed during the passage of a typhoon by a point is that D(CPA distance) and R_{50} (Radius of 50 kt winds) combine so that $D<R_{50}$. A particular verifying position (lat/lon) determines an instantaneous distance (D) from a known point. Hence the conditions for the 50 kt winds will be met by the typhoon occupying certain positions and at the same time having an R_{50} of a certain value. Each R_{50} and position can be expressed as a forecast and a particular error set (E-W error, N-S error and error in R_{50}). Given an initial value of R_{50}, the major contributor to determining R_{50} (and hence the R_{50} error) is the maximum wind. It is important then to examine the relationship between position errors and errors in maximum

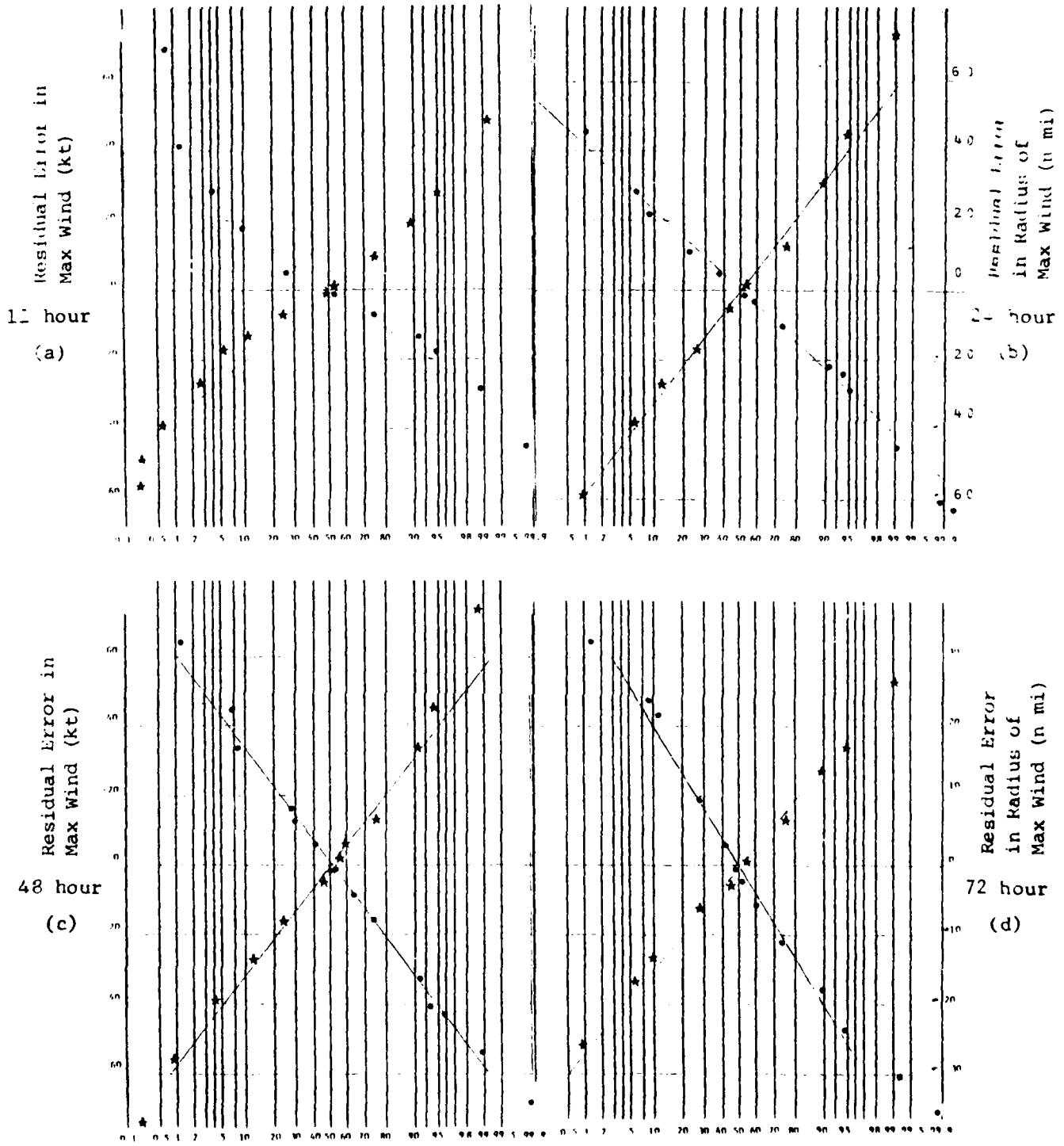

Figure 10. Plots of the cumulative frequency distributions of the residuals from the regression equations of Table 3 on probability paper. Left scale is residual of maximum wind (●), and right scale is residual of radius of maximum wind (★).

wind. Wind errors were compared to position errors for a sample consisting of the same cases as in Tables 1 and 2 but using only every fourth case to reduce interdependence. Table 4 summarizes the results of that comparison.

The components and vector position errors are consistent with those published by JTWC and found by others. The correlation between position error components (Rxy) is close to those found by Nicklin (1977), and the wind error is consistent with Table 1 except the overforecast bias is somewhat less in this sample.

The surprising finding here is the lack of correlation between position errors and wind errors. None of the Rxw, Ryw or Rea values are significantly non zero. One would have at least expected large errors in position to have been accompanied by large wind errors, but this does not seem to be the case. This finding is cited as the basis for the assumption that position errors and errors in the radius of a particular isotach are independent.

	12 hr	24 hr	48 hr	72 hr
Zonal error (W-E)X				
mean $\bar{X}$	-5 n mi	-5 n mi	-9 n mi	1 n mi
std dev Sx	58 n mi	116 n mi	233 n mi	378 n mi
Meridional (S-N) Y				
mean $\bar{Y}$	-5 n mi	-15 n mi	-40 n mi	-79 n mi
std dev Sy	49 n mi	93 n mi	187 n mi	269 n mi
Wind Error W				
mean $\bar{W}$	1 kt	2 kt	4 kt	3 kt
std dev Sw	13 kt	18 kt	24 kt	26 kt
Abs Wind Error A				
mean $\bar{A}$	9 kt	13 kt	19 kt	20 kt
std dev Sa	9 kt	12 kt	15 kt	17 kt
Position Vector Error E				
mean $\bar{E}$	65 n mi	130 n mi	262 n mi	405 n mi
std dev Se	40 n mi	74 n mi	149 n mi	240 n mi
Cases	504	390	293	203
Correlation Coefficients				
Rxy	0.03	0.09	0.23	0.33
Rxw	0.00+	-0.01	0.03	0.03
Ryw	-0.01	0.02	0.09	0.09
Rea	-0.00	-0.04	-0.07	0.07

Table 4 . Comparison of position forecast and wind forecast errors.

2.4 Computational Example

The actual operation of the model can best be described by means of an example.

The following nowcast and 24-hour forecast information is given:

	Time = 0	Time = 24
Latitude	12.5°N	13.6°N
Longitude	155.5°E	150.7°E
Maximum Wind (V_m)	105 kt	115 kt
Radius 50 kt wind	45 n mi	60 n mi
Radius 30 kt wind	90 n mi	120 n mi
Inferred R_m	9 n mi	10 n mi
Speed of motion	12 kt	
Past 12-hr change V_m	+10 kt	

Using the regression equation based on the coefficients from column 6, Table 3, the 24-hour maximum wind prediction (V^*) is 111 kt. The probabilities of the actual maximum winds falling within 7 discrete zones above 50 kts are shown as $P(V_1 \leq V_m < V_2)$ in Table 5.

Values of the radius of maximum winds are predicted using the regression coefficients of column 2, Table 3 and V_i, a representative value of V_m from each zone. Notice that in Table 3 the actual verifying V_m was

V_1 V_2	50 - 60		60 - 70		70 - 80		80 - 90		90 - 100		100 - 110		110 - ∞		SOURCE Assumed
$P(V_1 \leq V_m < V_2)$	.001		.005		.021		.069		.15		.231		.524		Regress Eqn Dist of Resid
V_i(kts)	55		65		75		85		95		105		119		
$R_m(V_i)$ n mi	51		46		41		35		30		24		16		Regression Equation
r_j	R_{ij}	P_{ij}	R_{ij}	P_{ij}	R_{ij}	P_{ij}	R_{ij}	P_{ij}	R_{ij}	P_{ij}	R_{ij}	P_{ij}	R_{ij}	P_{ij}	$P(R_{50} \geq r_j)$
25	21	.994	15	.995	11	.994	9	.985	7	.973	6	.933	4	.841	.897
50	41	.997	30	.908	22	.943	17	.933	14	.908	11	.860	9	.719	.801
75	62	.179	44	.568	33	.749	26	.773	21	.773	17	.719	13	.599	.665
100	83	.003	59	.140	44	.401	35	.500	28	.568	23	.532	18	.432	.479
125	103	.000	74	.010	56	.106	43	.251	35	.337	28	.371	22	.318	.323
150			89	.000	67	.015	52	.078	42	.159	34	.203	26	.203	.183
175					78	.001	61	.015	48	.067	40	.092	31	.106	.088
200					89	.000	69	.002	55	.019	45	.040	35	.057	.042
225							78	.000	62	.004	51	.012	40	.023	.015
250									69	.000	57	.003	44	.010	.006
275											68	.000	49	.004	.002
300													53	.001	.001
325													57	.000	.000

$$R_{ij} = \left(\frac{50}{V_i}\right)^2 r_j$$

$$P_{ij} = P(R_m \geq R_{ij}) = P(R_{50} \geq r_j \mid V_m = V_i)$$

$$P(R_{50} > r_j) = \sum_{\text{all } V_i} P\left(V_i - \frac{\Delta V}{2} < V_m < V_i + \frac{\Delta V}{2}\right) \cdot P(R_{50} > r_j \mid V_m = V_i)$$

Table 5. Sample computation of the co-cumulative probability of R_{50}.

was used as a predictor for R_m. Presently an array of assumed values of V_m (specifically V_i) are used to predict R_m. The predicted radii of maximum winds are shown as $R_M(V_i)$ in Table 5. Thirteen values of the radius of 50 kt winds (R_j), 25-325 n mi are assumed. Using the Riehl profile a radius of maximum winds (R_{ij}) is computed which would cause 50 kt winds to occur at radius R_j if V_m were V_i. P_{ij} is the probability the actual radius of maximum winds will exceed R_{ij} given the forecast $R_m(V_i)$. The column headed $P(R_{50}>R_j)$ is the sum of these probabilities weighted by $P(V_i<V_m<V_2)$.

This table of probabilities $P(R_{50}>R_j)$ can then be plotted graphically as in Figures 4c and 4e. Also needed for the plot in Figure 4e are the probabilities that the cyclone passes within a distance smaller than each of these R_j values $P(D<R_j)$. It is important to note that for over-water points the $P(R_{50}>R_j)$ are treated as being independent of geography, thus need only be calculated once irregardless of the variety of geographical points considered. The $P(D<R_j)$ are, of course, geography dependent.

2.5 Assymmetry

We assume the Riehl profile holds for both the right and left side of the cyclone and that the winds which are observed are the vector sum of the symmetric winds and the forward speed of motion.

If V_s is the stationary maximum wind located at radius R_m from the center, then the radius of some isotach V_c is given on the right side by

$$R_{cr} = \left(\frac{V_s + S}{V_c} \right)^2 R_m \ ,$$

and on the left by

$$R_{c\ell} = \left(\frac{V_s - S}{V_c} \right)^2 R_m \ ,$$

where S is the forward speed of motion. We assume the V_c isotach to be a circle of radius

$$R_c = \tfrac{1}{2}(R_{c\ell} + R_{cr}) \ ,$$

with center to the right of the cyclone at a distance

$$d_o = \tfrac{1}{2}(R_{cr} - R_{c\ell}) \ .$$

Simplifying

$$R_c = \frac{V_s^2 + S^2}{V_c^2} R_m = \frac{V_m^2 - 2S(V_m - S)}{V_c^2} R_m \ ,$$

and

$$d_o = \frac{2S\ V_s\ R_m}{V_c^2} = \frac{2S(V_m - S)}{V_c^2}\ R_m \quad ,$$

where

$$V_m = V_s + S.$$

To accomodate the offset we simply consider a point somewhat removed from the real point of concern. Because of the mirror image effect, that offset is to the left (relative to cyclone motion) of the point of concern. We then integrate over a symmetric area centered on this offset point. This space integration provides our estimate of $P(D<R_j)$.

2.6 Model Specifics

Most of the details of how the wind probability model works have been given. The basic equations to be solved are

$$P_{50} = \sum_{r_j=0}^{\infty} P(R_{50}>r_j) \cdot P(d=r_j)$$

and

$$P_{30} = \sum_{r_j=0}^{\infty} P(R_{30}>r_j) \cdot P(d=r_j)$$

over all values of r_j.

This is accomplished in the following eleven distinct operations.

(1) Select wind of concern V_c = 30 or 50 kts.

(2) Predict the maximum wind V_f (regression equation, Table 3).

(3) Assume in turn all reasonable values for maximum wind $V_i (V_i > V_c)$.

(4) Calculate the probability of each assumed wind occurring P_i ($P_i = P(V_i - 5 \leq V_i \leq V_i + 5)$).

(5) Predict a radius of maximum wind $R_m(V_i)$ (regression equation, Table 3 using V_i as a predictor).

(6) Assume in turn all reasonable values for the radius of V_c isotach r_j.

(7) Calculate the maximum wind radius R_{ij} necessary to cause the V_c isotach radius to be r_j if $V_m = V_i \ (R_{ij} + V_c/V_i)^2 r_j$).

(8) Calculate the probability of R_{ij} being exceeded (P_{ij}) given the forecast $R_m(V_i)$ (use residual from regression equation, Table 2).

(9) Add $P_{ij} \times P_{ij}$ on to a running sum of $P_j = P(R_c > r_j)$. These will be stored for the 0, 12, 24, 48 and 72 hour forecasts. (R_c is the actual verifying V_c isotach radius).

(10) When we consider a specific point (offset for assymmetry) we spatially integrate to obtain the probability of the cyclone passing within a radius (r_j, $P(D \leq r_j)$ similar to STRIKP) while interpolating from storage (see step 9) the probability

of this r_j being exceeded by the actual R_c. The sum of $P(D=r_j) \cdot P(R_c \geq r_j)$ over all possible r_j is the instantaneous probability of V_c winds occurring at our specified point.

(11) Integrate these probabilities over time in a manner identical to that of STRIKP.

The steps in the summations, which amount to finite differencing of the integrals of continuous functions, requires assumptions of end points and step spacing in operations 3, 6 and 10.

These decisions were made in part by first making the end points extremely far apart and the step spacing as fine as the data permitted (winds and radii are always specified in multiples of 5 kts or 5 n mi). Thereafter, in the interest of economy of operation, these were relaxed so long as no significant differences were evident in the probabilities for a test set of cases.

The limits and steps in the final version of WINDP are as follows:

V_c : 30 or 50 kts

V_m : V_c to 150 kts in 10 kt steps

R_c : 0 to 675 n mi in 75 n mi steps

r_j : 0.5 Sy to 675 n mi in 0.5 Sy steps, where Sy is the standard deviation of the north-south component of forecast error.

2.7 Testing

All aspects of the WINDP/STRIKP programs were tested on independent data. Generally the test results show the principles to be sound and the weaknesses to be minor and manageable by routine monitoring.

2.7.1 Has the track forecast accuracy changed from that of the base years? A major improvement in track forecasting would invalidate WINDP/STRIKP since an underlying assumption has been that forecast errors have not changed statistically over the past decade. Figure 11 shows adjusted or handicapped average annual forecast errors for the years 1966-79. These are adjusted for forecast difficulty and reconnaissance support (see Jarrell et al, 1978). There does appear to be a trend toward decreasing forecast errors. Our purpose in examining the trend in forecast errors is to project into the future and to estimate whether or not adjustments should be made for the trend. The adjustment for difficulty is reasonable because we can't anticipate forecast difficulty on a long term basis. The adjustment for reconnaissance, on the other hand, is inappropriate for the present purpose since it contributes to the trend in a non-random and fairly predictable way. It is clear that the trend would be somewhat offset without the adjustment for reconnaissance support since this adjustment has grown steadily since it reached a minimum in 1968-69. The slope of the 24-hour trend line in Figure 11 shows a 1.2 nmi/year improvement, which is small but significant (α=0.05). The same slope without the reconnaissance adjustment is 0.27 nmi/year improvement; the latter is not significant (α=.05). This suggests that real improvement in forecasting skill is being essentially offset by poorer positioning capability within the warning/forecast system.

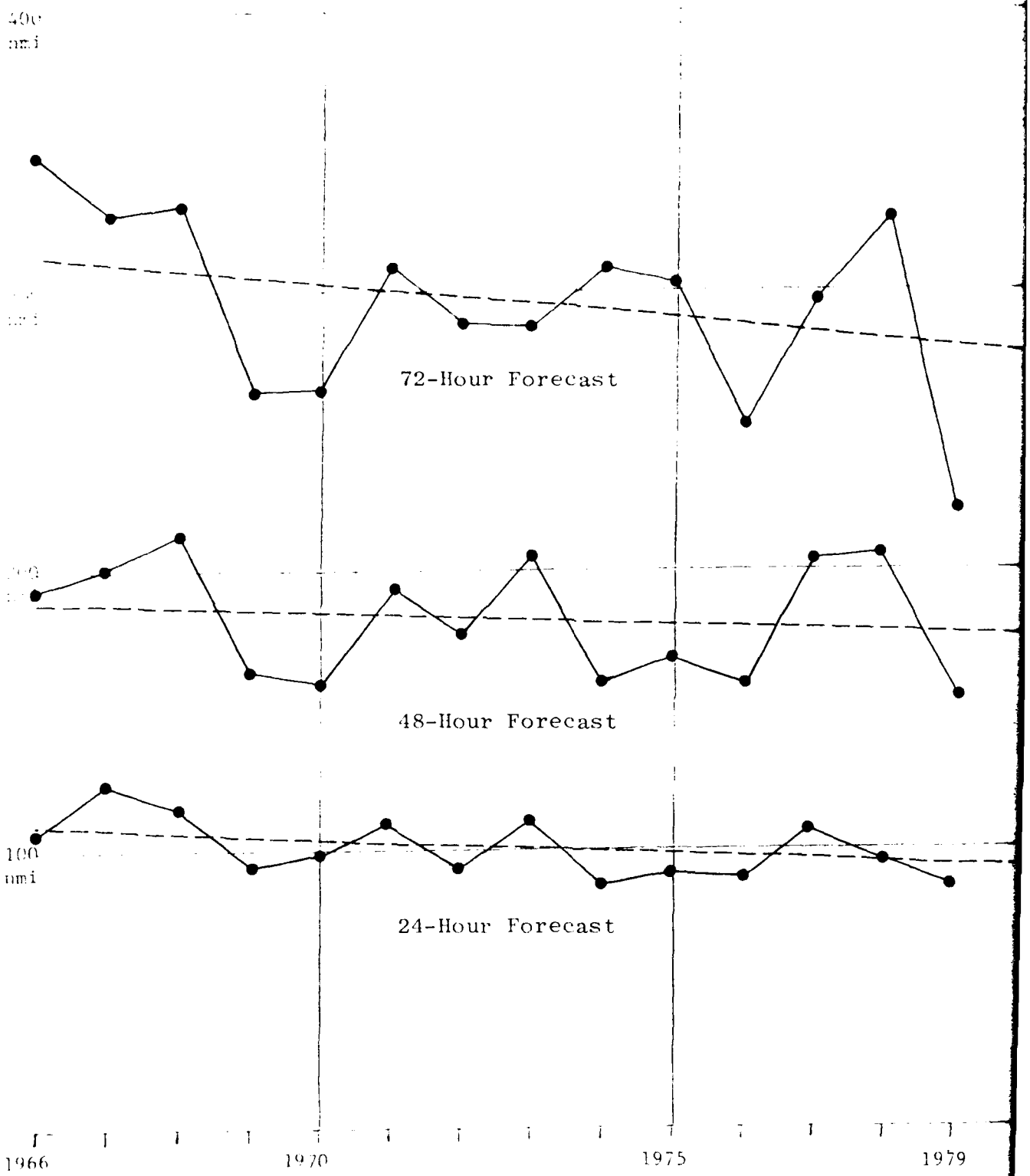

Figure 11. 1966-79 annual forecast errors adjusted for difficulty and reconnaissance support (after Jarrell et al 1978). The dashed lines are least squares trend lines.

Figure 12 compares the way the 1979 forecasts fit the STRIKP bivariate normal model. One can think of a vertical line as representing a probability ellipse, where that line intersects the 45° line is the fraction of the verifying positions which were expected to fall within the ellipse. The string of dots represents what really happened. Dots below the line represent worse than expected forecasts, those above are better than expected. As can be seen, the relatively easy (Class 1) forecasts were handled slightly worse than their historical (1966-75) counterpart while the average (Class 2) and difficult (Class 3) forecasts were forecast better than their historical counterparts. This finding is consistent with the conclusion above, concerning reconnaissance, since the easy forecasts are most persistent and hence most susceptible to tracking error. One cannot directly apply the results of Figure 12 to evaluate the wind/strike probabilities since these are very specialized probabilities centered on the forecast point. The implication is that for Class 2 and particularly Class 3 cases, probability ellipses would be too big; this results in probabilities for points far off the track being too large (small probabilities are too large) and those along the track being too small (large probabilities are too small). Since Figure 11 shows 1979 to have been an unusually well forecast year, it does not appear reasonable to expect a continued trend of well handled Class 2 and Class 3 forecasts; no adjustment for trend appears warranted based on the observation that the trend in forecast errors is near zero.

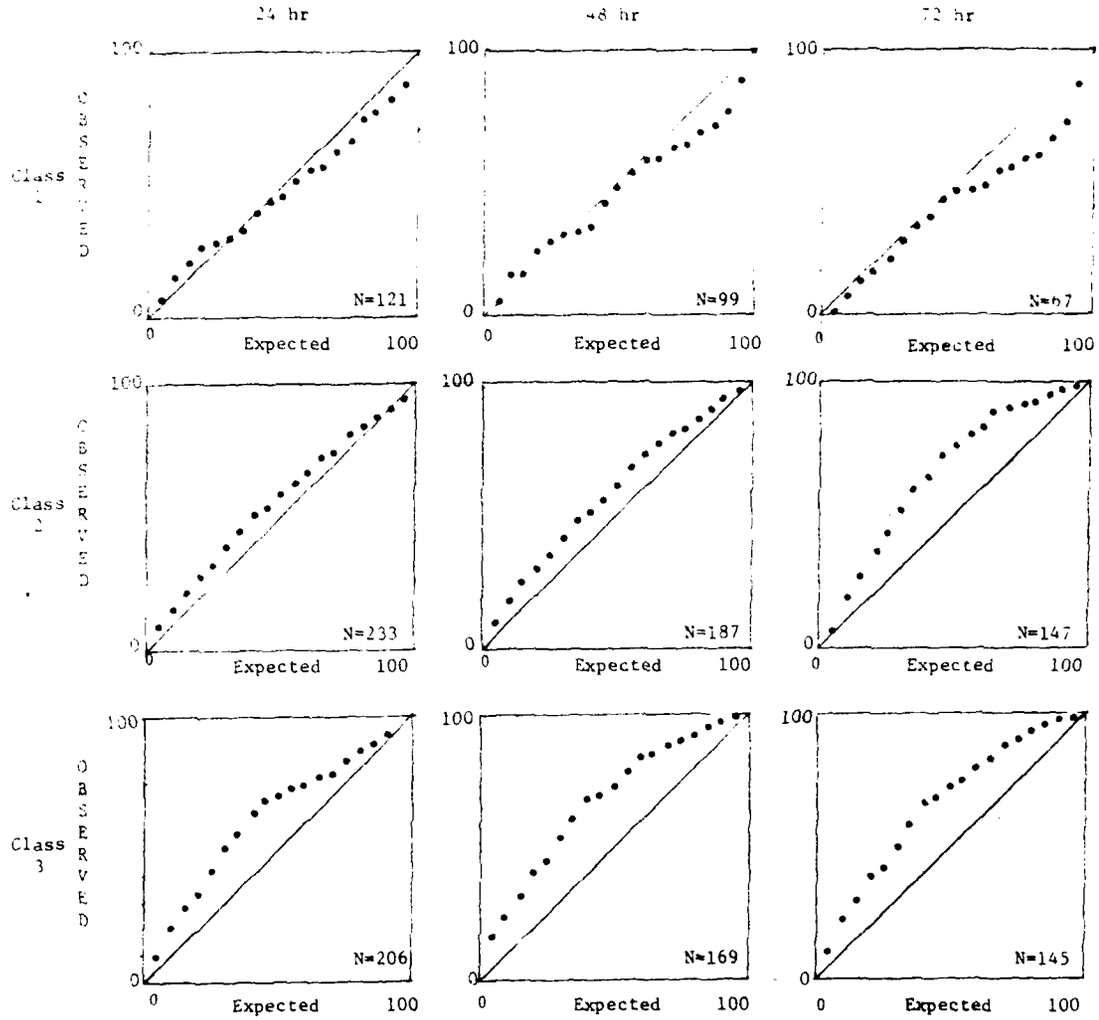

Figure 12. Comparison of distribution of Western Pacific tropical cyclone forecast errors to bivariate normal distributions described by Nicklin (1978). Individual diagrams are left to right for 24, 48 and 72 hour forecasts and top to bottom for class 1, 2 and 3 forecasts which are expected (in advance) to be easy, average and difficult respectively.

2.7.2 Testing of wind and wind radii forecasts.

The maximum wind and wind radii were verified against best track (maximum wind) and warning data (radii) for 1979. The wind radius verified is the circular average of that forecast or reported.

The following table summarizes the verification.

Fcst Interval (hrs)	Max Winds Mean Error(kt)	Max Winds STD Dev(kt)	30 kt Radius Mean Error(nm)	30 kt Radius STD Dev(nm)	50 kt Radius Mean Error(nm)	50 kt Radius STD Dev (nm)	Cases
12	-1	13			-1	23	608
24	-2	18	-1	58	-2	30	559
48	-2	26			-2	38	455
72	0	32			-2	43	359

Table 6.

Comparable figures for the maximum winds (no comparable wind radius data were computed) for the dependent development data are:

Interval	Mean	Stdev
12 hr	2 kts	15 kts
24 hr	3 kts	20 kts
48 hr	5 kts	28 kts
72 hr	12 kts	33 kts

It is apparent that the large bias which was evident in the development data has been removed. Since the WINDP algorithm anticipates and corrects for this bias, there is a danger that winds will be underforecast. As will be shown, this does not appear to be the case. The intercept for the wind regression equations (in the wind radius algorithm) could be increased by the mean above, in effect, assuming a zero bias. No comparable adjustment would be necessary for wind radii since they are heavily dependent on max wind. This adjustment does not appear warranted since no systematic underforecast (of WINDP) is observed. Maximum wind impacts WINDP (a) in establishing the probability that 30 or 50 kt winds exist at all and (b) through its influence on the wind radii. The importance of the latter input is minimized because maximum wind enters through a regression equation (for radius of maximum wind) where its effect is tempered with other predictors.

A far more important aspect of the verification of maximum winds and radii is the behavior of the wind radius algorithm. The fundamental assumption was that errors out of this algorithm are normally distributed. Figure 13 shows a comparison of the cumulative distribution of errors against the normal model. As with figure 12, the intersection of a vertical line with the 45° line represents the expected, while the dots represent the observed. The agreement of the maximum wind to the model is nearly perfect, as is the 30 kt wind radius comparison which has no points where the difference between observed and expected is significant (α=0.05). There are some points on the 50 kt radius where the difference in observed and expected are significantly different. These are around 40% on the 12 and 24 hour comparisons; note that these are back near the

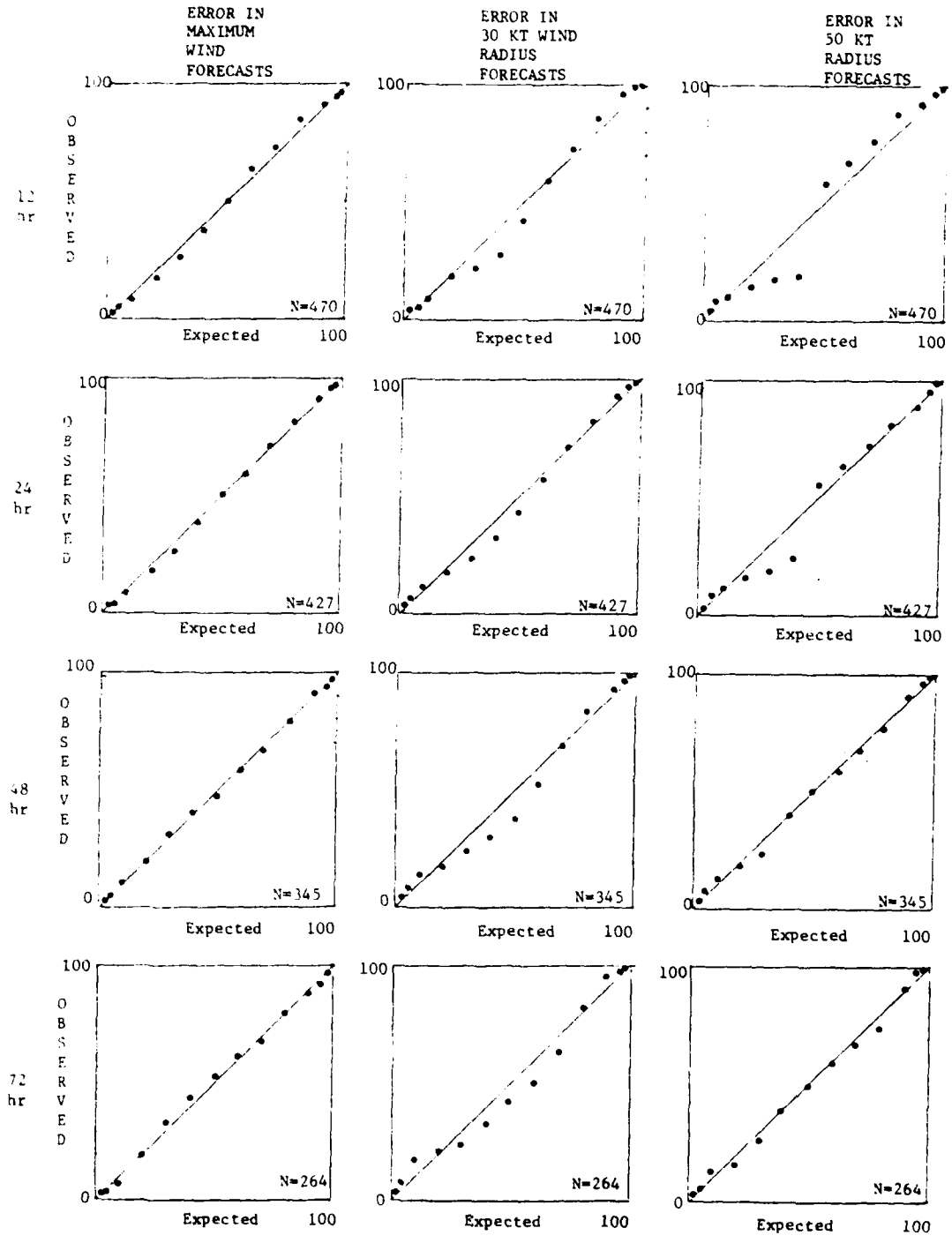

Figure 13.
Comparison of forecast error cumulative distribution to a normal distribution. Individual diagrams are left to right maximum wind error, 30 kt wind radius error and 50 kt wind error. Top to bottom are forecast times 12, 24, 48 and 72 hours.

line by 50%. This represents a spike of correct forecasts (a spike on a bell shaped curve). There is no easy answer for why this occurs, and it may be related to a prediction (and verification) of radius = zero, which is the case when the maximum winds are below 50 kts.

2.7.3 Discrimination Based on Warning Position Error (WPE). The forecast difficulty algorithm does not directly consider WPE. Indirectly this may be considered since WPE is related to several other predictors (i.e., maximum wind, latitude, speed of motion, etc.). Two methods of estimating WPE were tried; these were:

(1) relating WPE to "accurate within" figure in the warning, and

(2) relating WPE to fix basis as given in the warning.

The second method is far better and it alone will be discussed here. First, all 1979 forecasts were divided into unique classes on fix basis. For example, one class was aircraft reconnaissance, another was land radar, another combined these two, etc. WPEs were computed for each class and classes were combined where WPEs appeared to be about the same.

The first group to fall out were the bad positions. When the terms "extrapolation", "synoptic" or "ship" data were used, WPEs as a group were large (Class C). When

aircraft, or land radar was cited (without citing also any of the previous three methods), WPEs tended to be small (Class A). All other combinations, which were dominated by satellite fixes, were left to a large middle group (Class B). Table 7 relates mean WPE (nmi) stratified by fix class (A,B,C) and difficulty class (1,2,3) as a ratio to those currently in the WINDP/STRIKP models. These involve 1084 cases from both 1978 and 1979 forecasts.

	DIFFICULTY CLASS			
Fix Class	1	2	3	ALL
A	12 (64)	18 (68)	15 (121)	15 (253)
B	23 (159)	27 (279)	26 (332)	26 (770)
C	27 (7)	31 (25)	35 (29)	32 (61)
	20 (230)	26 (372)	24 (482)	21 (1084)

Table 7. Average Warning Position Errors (WPE) as a function of difficulty class (1,2 or 3) and fix class (A,B or C). Errors are given in nmi. The average WPE in the STRIKP development sample (1971-1975) was about 26 nmi. Figures in paranthesis are numbers of cases.

This information could be used to modify the existing bivariate normal parameters in any of several ways. Care must be exercised not to go overboard on this relatively small data set (the 66-75 data set was about 5000 cases). One conservative method of applying this data is to adjust the standard deviations (in the STRIKP algorithm) according to variation in average error as a function of forecast period (0-72 hours), difficulty class and fix class. This would improve discrimination and should lead to better probability estimates (increased large values, decreased small values). Figure 14 illustrates a least square

fit (over time) to suitable adjustment factors. This figure suggests that with the easy (Class 1) forecasts, the better the warning position, the better the forecast. With the more difficult classes the previous appears only to hold true in the short range forecasts (less than 36 hours); for longer range forecasts the worse the WPE, the better the forecast error. This, apparent paradox may relate to the necessity to "forecast" with these difficult cases versus using extrapolation. This argument only holds up if we assume the forecaster knows he has a difficult forecast and understands the quality of his warning position. Recognizing a difficult forecast has been facilitated by the STRIKP program providing difficulty class information over the 1978-79 seasons. A module to adjust standard deviations for difficulty class/fix class combinations was placed in the STRIKP code and forecast confidence values were computed. Those confidence values are given in Table 8.

Conclusion. The testing of WPE indicates a strong potential for improving the discrimination by using fix class. Because this was a limited data set, further testing is recommended prior to a decision on adoption of this (or some similar) algorithm modification.

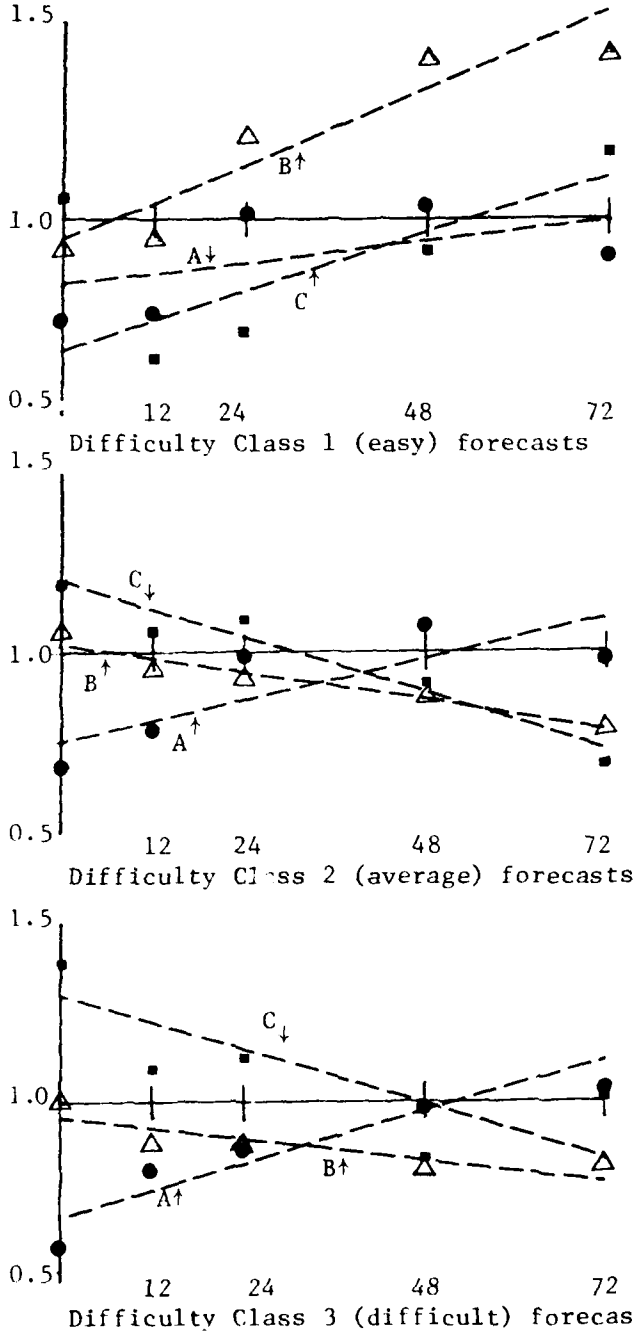

Figure 14. Average forecast error of 1978-79 tropical cyclones as a function of difficulty class (1,2, and 3) and fix class A(●), B(△) and C(■). Errors are given as a ratio to the average error for that difficulty class in the STRIKP development sample (1966-75). (- - - are least squares fit lines). On the left scale 1.5 would be 50% larger than the corresponding average error in the development sample

FORECAST CLASS		1			2			3		
Fix Class		A	B	C*	A	B	C	A	B	C
Time	Dist (nmi)	%	%	%	%	%	%	%	%	%
0	20	60	35	35	48	30	23	55	34	20
	30	87	62	62	77	55	45	83	60	40
12	50	56	34	34	34	25	20	31	22	13
	75	84	60	60	60	47	39	56	42	27
24	100	65	41	41	40	35	30	33	29	19
	150	90	69	69	68	61	54	58	53	37
48	200	43	26	26	32	39	37	24	31	23
	300	71	51	51	58	67	65	47	57	45
72	300	30	18	18	27	43	49	21	38	33
	450	55	64	64	49	74	77	41	66	60

Table 8. Estimates of probability that forecast errors classified by fix type and difficulty class, be less than two distances. (Note the second probability includes the first.)
*Only two fix classes are recognized for Class 1 forecasts, Class C was so small it was merged with Class B.

2.7.4 Testing WINDP. Testing of the WINDP predicted values against observed followed the same plan as with STRIKP reported by Jarrell (1978). An array of latitude/longitude coordinates of 40 western Pacific points (Figure 15) was assembled. WINDP values for 30 and 50 kts were calculated at 12 hour intervals from the issue time of 1978 and 1979 JTWC tropical cyclone forecasts. Points of computation were selected at random from the array of forty for each storm so not more than 10 points were considered for any storm and these were further reduced by using only those which would eventually be within 1000 miles of the tropical cyclone being forecast (using hindsight). A hit was assumed if the calculated warning time probability was greater than 50% (an alternate but more computationally complex method which determined if the point was within the nowcast radii about a best track point gave virtually identical results). As a special case verifying positions which had a best track wind of at least 30 kts but no 30 kt wind radius or less than 30 kt winds with a non-zero 30 kt radius were considered conflicting information and not used to verify the occurrence of 30 kt winds but were used to verify 50 kt winds. A similar situation occurs relative to 50 kt winds. Since 30 kt winds are a typical maximum reported for the tropical depression stage this first condition occurred frequently. For this reason there are more verifiable 50 kt WINDP predictions than 30 kt even though both can always be computed.

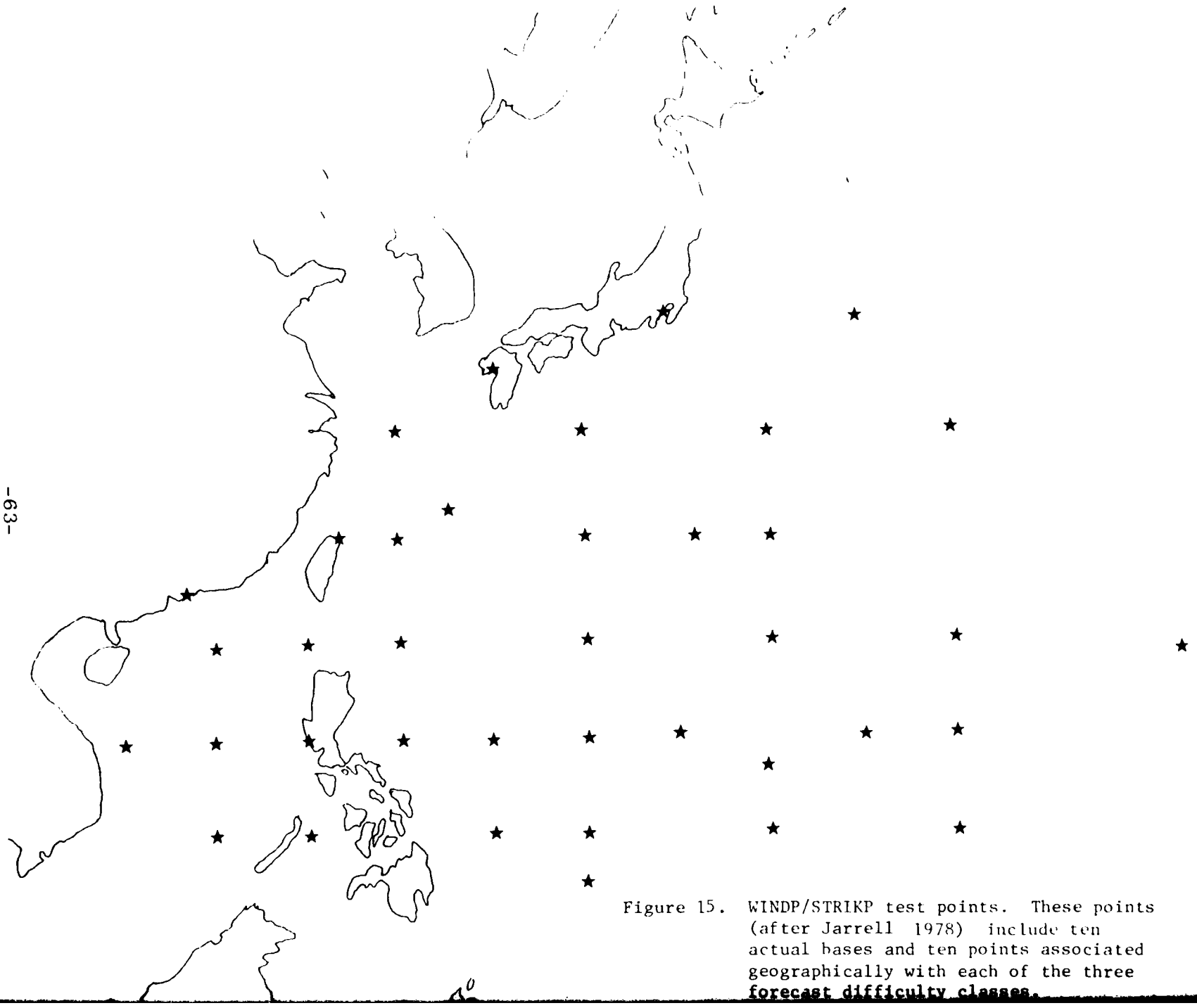

Figure 15. WINDP/STRIKP test points. These points (after Jarrell 1978) include ten actual bases and ten points associated geographically with each of the three forecast difficulty classes.

Table 9 compares the observed occurrences of 30 or 50 kt winds to the expected number of occurrences. The latter is calculated by the sum of the instantaneous probabilities in class cells of increasing width (B-A).

	24 Hour			48 Hour			72 Hour		
A - B	EXP	OBS	CASES	EXP	OBS	CASES	EXP	OBS	CASES
0 - 12	0	7*	1213	1	9*	635	0	9*	290
12 - 24	1	1	124	1	2	166	1	3	160
24 - 36	3	1	114	4	1	155	3	6	139
36 - 48	6	4	108	9	5	169	8	13	158
48 - 60	10	3	87	19	21	172	20	14	178
60 - 120	29	15	127	39	21	177	30	26	138
120 - 240	58	41	122	41	34	96	6	5	15
240-100	22	22	30	1	0	1	1	0	1
ALL	129	94	1925	115	93	1571	69	76	1079

Table 9.

The comparison is generally quite good, but does tend toward overforecasting probability. A rather shocking number of observed cases of 30 kt winds followed very small probabilities (0-12). Note that one forecast may occur several times and that 24 of these 25 occurrences (7+9+9) are all associated with one cyclone (ABBY 1979) and a short series of forecasts of fast westward motion which preceded a sharp turn to a fast eastnortheast track. This verifying track happened to pass several test points. The point here is that in reality, this is not 24 forecasts, but only one independent non recurvature forecast which busted. Because establishing independence between cases is difficult there is no valid test for the significance of the

SUMMARY

The testing revealed two weaknesses which one might conclude would lead to biased probability estimates. The correction of an earlier wind overforecasting bias would seem to cause underforecasting WINDP. The better forecasting (although likely not a trend) in the independent data would suggest overforecasting the small probabilities (offsetting the above) while underforecasting the large probabilities (reinforcing the above). Thus we would at the very least expect to see the large values underforecast, but instead we seem to see a general overforecast. There appears to be no compelling argument to support any empirical adjustment to correct deficiencies whose significance is marginal.

There does appear to be merit to discriminating forecast difficulty on the basis of WPE as estimated by fix source. It is recommended that this concept be tested on 1980 forecasts. If the JTWC has retained difficulty class specifications for 1980 forecasts, a reasonable test on forecast error could be readily conducted using Table 8 without additional outside effort. Because some implications of these discrimination results represent a departure from the expected, further independent testing should be conducted before a decision to adopt WPE discrimination into the WINDP/STRIKP algorithm is finalized. Such adaption is a minor programming effort. In any case WPE discrimination offers a further, although tentative, aid to JTWC's confidence estimating efforts.

Test results for the time integrated probabilities are much the same. The following table compares occurrences versus expected 30 and 50 kt winds over 12 hour periods. None of these are significantly different using the same 5% test as before although the 48-60 hour 30 kt comparison is borderline.

	30 KT			50 KT		
Period (hours)	EXP	OBS	CASES	EXP	OBS	CASES
0-12	93	60	624	26	16	756
12-24	69	43	550	23	17	682
24-36	39	29	561	14	9	672
36-48	35	39	351	14	16	318
48-60	13	0	459	12	10	413
60-72	15	20	258	7	12	235

Table 11.

These show the same tendency to overforecast as do the instantaneous predictions. The one plausible explanation for this phenomena is that the test forecasts were better than expected. This is particularly true of the long range forecasts. Good forecasting results in an overestimate of probabilities relative to points far removed from the track (small probabilities) and an underestimate of large probabilities. As can be seen from Tables 9 and 10, large probabilities are rare with long range forecasts. For this reason there is an apparent overforecasting tendency which is considered to be transitory, associated with 1979 only.

SUMMARY

The testing revealed two weaknesses which one might conclude would lead to biased probability estimates. The correction of an earlier wind overforecasting bias would seem to cause underforecasting WINDP. The better forecasting (although likely not a trend) in the independent data would suggest overforecasting the small probabilities (offsetting the above) while underforecasting the large probabilities (reinforcing the above). Thus we would at the very least expect to see the large values underforecast, but instead we seem to see a general overforecast. There appears to be no compelling argument to support any empirical adjustment to correct deficiencies whose significance is marginal.

There does appear to be merit to discriminating forecast difficulty on the basis of WPE as estimated by fix source. It is recommended that this concept be tested on 1980 forecasts. If the JTWC has retained difficulty class specifications for 1980 forecasts, a reasonable test on forecast error could be readily conducted using Table 8 without additional outside effort. Because some implications of these discrimination results represent a departure from the expected, further independent testing should be conducted before a decision to adopt WPE discrimination into the WINDP/STRIKP algorithm is finalized. Such adaption is a minor programming effort. In any case WPE discrimination offers a further, although tentative, aid to JTWC's confidence estimating efforts.

BIBLIOGRAPHY

Brody, L.R., Brand, S., Jarrell, J.D., and Tsui, T., 1979: Statistical studies using unique western Pacific tropical cyclone wind radii data, Twelfth Technical Conference on Hurricanes and Trop. Met., New Orleans, April 24-27, 1979.

Jarrell, J.D., 1978: Tropical Cyclone Strike Probability Forecasting, Naval Environmental Prediction Research Facility Contractor Report CR 78-01.

Jarrell, J.D., Brand, S., and Nicklin, D.S., 1978: An analysis of western North Pacific tropical cyclone forecast errors, Mon. Wea. Rev., 106.

Joint Typhoon Warning Center, 1977: Annual typhoon report 1977. Fleet Weather Central/Joint Typhoon Warning Center.

Nicklin, D.S., 1977: A Statistical Analysis of Western Pacific Tropical Cyclone Forecast Errors, M.S. Thesis, U.S. Naval Postgraduate School.

Riehl, H., 1963: Some relations between wind and thermal structure of steady state hurricanes, J. Atmos. Sci., 20, 276-287.

COMMANDER IN CHIEF
U.S. ATLANTIC FLEET
NORFOLK, VA 23511

COMMANDER IN CHIEF
U.S. ATLANTIC FLEET
(N009/04E)
ATTN: NSAP SCIENCE ADVISOR
NORFOLK, VA 23511

COMMANDER IN CHIEF
U.S. PACIFIC FLEET
PEARL HARBOR, HI 96860

COMMANDER
SECOND FLEET
FPO NEW YORK 09501

COMMANDER
THIRD FLEET
PEARL HARBOR, HI 96860

COMMANDER
SEVENTH FLEET (N30W)
ATTN: FLEET METEOROLOGIST
FPO SAN FRANCISCO 96601

COMTHIRDFLT
ATTN: NSAP SCIENCE ADVISOR
CODE N702/01T
PEARL HARBOR, HI 96860

COMSEVENTHFLT
ATTN: NSAP SCIENCE ADVISOR
BOX 167
FPO SEATTLE 98762

COMMANDER
U.S. NAVAL FORCES, CARIBBEAN
FPO MIAMI 34051

COMMANDER
NAVAL AIR FORCE
U.S. ATLANTIC FLEET (30F)
ATTN: NSAP SCIENCE ADVISOR
NORFOLK, VA 23511

COMMANDER
NAVAL AIR FORCE
U.S. PACIFIC FLEET
ATTN: NSAP SCIENCE ADVISOR
NAS, NORTH ISLAND
SAN DIEGO, CA 92135

COMMANDER
NAVAL SURFACE FORCE
U.S. PACIFIC FLEET (OG5/N6N)
ATTN: NSAP SCIENCE ADVISOR
NAVAL AMPHIBIOUS BASE, CORONADO
SAN DIEGO, CA 92155

COMMANDER
SUBMARINE FORCE
U.S. ATLANTIC FLEET
ATTN: NSAP SCIENCE ADVISOR
NORFOLK, VA 23511

COMMANDER
AMPHIBIOUS GROUP 2
ATTN: METEOROLOGICAL OFFICER
FPO NEW YORK 09501

COMMANDER
AMPHIBIOUS GROUP 1
ATTN: METEOROLOGICAL OFFICER
FPO SAN FRANCISCO 96601

COMMANDING OFFICER
USS AMERICA (CV-66)
ATTN: MET. OFFICER
FPO NEW YORK 09531

COMMANDING OFFICER
USS FORRESTAL (CV-59)
ATTN: MET. OFFICER
FPO MIAMI 34080

COMMANDING OFFICER
USS INDEPENDENCE (CV-62)
ATTN: MET. OFFICER
FPO NEW YORK 09537

COMMANDING OFFICER
USS J. F. KENNEDY (CV-67)
ATTN: MET. OFFICER
FPO NEW YORK 09538

COMMANDING OFFICER
USS NIMITZ (CVN-68)
ATTN: MET. OFFICER
FPO NEW YORK 09542

COMMANDING OFFICER
USS EISENHOWER (CVN-69)
ATTN: MET. OFFICER
FPO NEW YORK 09532

COMMANDING OFFICER
USS SARATOGA (CV-60)
ATTN: MET. OFFICER
FPO NEW YORK 09587

COMMANDING OFFICER
USS CONSTELLATION (CV-64)
ATTN: MET. OFFICER
FPO SAN FRANCISCO 96635

COMMANDING OFFICER
USS OCRAL SEA (CV-43)
ATTN: MET. OFFICER
FPO SAN FRANCISCO 96632

COMMANDING OFFICER
USS ENTERPRISE (CVN-65)
ATTN: MET. OFFICER
FPO SAN FRANCISCO 96636

COMMANDING OFFICER
USS KITTY HAWK (CV-63)
ATTN: MET. OFFICER
FPO SAN FRANCISCO 96634

COMMANDING OFFICER
USS MIDWAY (CV-41)
ATTN: MET. OFFICER
FPO SAN FRANCISCO 96631

COMMANDING OFFICER
USS RANGER (CV-61)
ATTN: MET. OFFICER
FPO SAN FRANCISCO 96633

COMMANDING OFFICER
USS MOUNT WHITNEY (LCC-20)
ATTN: MET. OFFICER
FPO NEW YORK 09517

COMMANDING OFFICER
USS BLUE RIDGE (LCC-19)
ATTN: MET. OFFICER
FPO SAN FRANCISCO 96628

COMMANDING OFFICER
USS GUADALCANAL (LPH-7)
ATTN: MET. OFFICER
FPO NEW YORK 09562

COMMANDING OFFICER
USS GUAM (LPH-9)
ATTN: MET. OFFICER
FPO NEW YORK 09563

COMMANDING OFFICER
USS INCHON (LPH-12)
ATTN: MET. OFFICER
FPO NEW YORK 09529

COMMANDING OFFICER
USS IWO JIMA (LPH-2)
ATTN: MET. OFFICER
FPO NEW YORK 09561

COMMANDING OFFICER
USS NEW ORLEANS (LPH-11)
ATTN: MET. OFFICER
FPO SAN FRANCISCO 96627

COMMANDING OFFICER
USS OKINAWA (LPH-3)
ATTN: MET. OFFICER
FPO SAN FRANCISCO 96625

COMMANDING OFFICER
USS TRIPOLI (LPH-10)
ATTN: MET. OFFICER
FPO SAN FRANCISCO 96626

COMMANDING OFFICER
USS TARAWA (LHA-1)
ATTN: MET. OFFICER
FPO SAN FRANCISCO 96622

COMMANDING OFFICER
USS NASSAU (LHA-4)
ATTN: MET. OFFICER
FPO NEW YORK 09557

COMMANDING OFFICER
USS SAIPAN (LHA-2)
ATTN: MET OFFICER
FPO NEW YORK 09549

COMMANDING OFFICER
USS BELLEAU WOOD (LHA-3)
ATTN: MET. OFFICER
FPO SAN FRANCISCO 96623

COMMANDING OFFICER
USS PUGET SOUND (AD-38)
ATTN: MET. OFFICER
FPO NEW YORK 09544

COMMANDING OFFICER
USS LASALLE (AGF-3)
ATTN: MET. OFFICER
FPO NEW YORK 09577

COMMANDING OFFICER
USS POINT LOMA (AGDS-2)
ATTN: MET. OFFICER
FPO SAN FRANCISCO 96677

COMMANDER IN CHIEF ATLANTIC
NAVAL BASE
NORFOLK, VA 23511

COMMANDER IN CHIEF PACIFIC
BOX 13
STAFF CINCPAC J37
CAMP SMITH, HI 96861

SPECIAL ASST. TO THE ASST.
SECNAV (R&D)
ROOM 4E741
THE PENTAGON
WASHINGTON, DC 20360

CHIEF OF NAVAL RESEARCH
LIBRARY SERVICES, CODE 734
RM 633, BALLSTON TOWER #1
800 QUINCY STREET
ARLINGTON, VA 22217

OFFICE OF NAVAL RESEARCH
CODE 465
ARLINGTON, VA 22217

CHIEF OF NAVAL OPERATIONS
OP-952
NAVY DEPT.
WASHINGTON, DC 20350

CHIEF OF NAVAL OPERATIONS
OP-986
NAVY DEPT.
WASHINGTON, DC 20350

WEATHER ELEMENT
NATIONAL MILITARY COMMAND
CENTER, THE PENTAGON
RM 2D921H
WASHINGTON, DC 20301

DEPUTY DIRECTOR FOR OPERATIONS
(ENVIRONMENTAL SERVICES)
OJCS, RM 1B679
THE PENTAGON
WASHINGTON, DC 20301

DET 2, HQ AWS
THE PENTAGON
WASHINGTON, DC 20330

NAVAL DEPUTY TO THE ADMIN.
NOAA, RM 200, PAGE BLDG. #1
3300 WHITEHAVEN ST. NW
WASHINGTON, DC 20235

OFFICER IN CHARGE
NAVOCEANCOMDET, BOX 81
U.S. NAVAL AIR STATION
FPO SAN FRANCISCO 96637

OFFICER IN CHARGE
NAVOCEANCOMDET
FEDERAL BLDG.
ASHEVILLE, NC 28801

OFFICER IN CHARGE
NAVOCEANCOMDET
U.S. NAVAL AIR FACILITY
FPO SEATTLE 98767

OFFICER IN CHARGE
NAVOCEANCOMDET
NAVAL AIR STATION
BARBERS PT., HI 96862

CPOIC
NAVOCEANCOMDET, CHASE FIELD
BEEVILLE, TX 78103

OFFICER IN CHARGE
NAVOCEANCOMDET
U.S. NAVAL AIR STATION
FPO NEW YORK 09560

OFFICER IN CHARGE
NAVOCEANCOMDET
NAVAL AIR STATION
CECIL FIELD, FL 32215

OFFICER IN CHARGE
NAVOCEANCOMDET
NAVAL STATION
CHARLESTON, SC 29408

OFFICER IN CHARGE
NAVOCEANCOMDET
NAVAL AIR STATION
CORPUS CHRISTI, TX 78419

OFFICER IN CHARGE
NAVOCEANCOMDET, BOX 63
U.S. NAVAL AIR STATION
FPO SAN FRANCISCO 96654

OFFICER IN CHARGE
US NAVOCEANCOMDET
BOX 16
FPO NEW YORK 09593

OFFICER IN CHARGE
NAVOCEANCOMDET
BOX 9048
NAVAL AIR STATION
KEY WEST, FL 33040

CPOIC
NAVOCEANCOMDET
NAVAL AIR STATION
KINGSVILLE, TX 78363

CPOIC
NAVOCEANCOMDET
NAVAL AIR STATION
MAYPORT, FL 32228

OFFICER IN CHARGE
NAVOCEANCOMDET
NAS, WHITING FIELD
MILTON, FL 32570

OFFICER IN CHARGE
NAVOCEANCOMDET
NAVAL AIR STATION
MERIDIAN, MS 39301

OFFICER IN CHARGE
NAVOCEANCOMDET
U.S. NAVAIRFAC, BOX 35
FPO SAN FRANCISCO 96614

OFFICER IN CHARGE
US NAVOCEANCOMDET
APO SAN FRANCISCO 96519

OFFICER IN CHARGE
NAVOCEANCOMDET
AIR FORCE GLOBAL WEATHER CENTRAL
OFFUTT AFB, NE 68113

CPOIC
NAVOCEANCOMDET
NAVAL AIR STATION
NEW ORLEANS, LA 70146

OFFICER IN CHARGE
NAVOCEANCOMDET
NAVAL AIR STATION
PATUXENT RIVER, MD 20670

OFFICER IN CHARGE
NAVOCEANCOMDET
U.S. NAVAL STATION
FPO MIAMI 34051

OFFICER IN CHARGE
NAVOCEANCOMDET
NAS, OCEANA
VIRGINIA BEACH, VA 23460

OFFICER IN CHARGE
US NAVOCEANCOMDET
FPO SAN FRANCISCO 96685

OFFICER IN CHARGE
US NAVOCEANCOMDET
FLEET ACTIVITIES
FPO SEATTLE 98770

OFFICER IN CHARGE
NAVOCEANCOMDET
NAVAL AIR STATION
PENSACOLA, FL 32508

OFFICER IN CHARGE
NAVOCEANCOMDET
MONTEREY, CA 93940

COMMANDING OFFICER
NORDA, CODE 101
NSTL STATION
BAY ST. LOUIS, MS 39529

COMMANDER
NAVAL OCEANOGRAPHY COMMAND
NSTL STATION
BAY ST. LOUIS, MS 39529

COMMANDING OFFICER
NAVOCEANO, LIBRARY
NSTL STATION
BAY ST. LOUIS, MS 39522

COMMANDING OFFICER
FLENUMOCEANCEN
MONTEREY, CA 93940

COMMANDING OFFICER
NAVWESTOCEANCEN
BOX 113
PEARL HARBOR, HI 96860

COMMANDING OFFICER
NAVEASTOCEANCEN
MCADIE BLDG. (U-117)
NAVAL AIR STATION
NORFOLK, VA 23511

COMMANDING OFFICER
US NAVOCEANCOMCEN
BOX 12
COMNAVMARIANAS
FPO SAN FRANCISCO 96630

COMMANDING OFFICER
NAVOCEANCOMFAC
NAS, P.O. BOX 85
JACKSONVILLE, FL 32212

COMMANDING OFFICER
US NAVOCEANCOMFAC
FPO SEATTLE 98762

SUPERINTENDENT
LIBRARY REPORTS
U.S. NAVAL ACADEMY
ANNAPOLIS, MD 21402

PRESIDENT
NAVAL WAR COLLEGE
ATTN: LCDR M. E. GIBBS
NEWPORT, RI 02840

U.S. NAVAL OBSERVATORY
ATTN: DR. R. W. JAMES
OPNAV 952D1
34TH & MASSACHUSETTS AVE. NW
WASHINGTON, DC 20390

COMMANDER
NAVAIRSYSCOM
ATTN: LIBRARY, AIR-00D4
WASHINGTON, DC 20361

COMMANDER
NAVAIRSYSCOM, AIR-370
WASHINGTON, DC 20361

COMMANDER
NAVAIRSYSCOM, AIR-553
MET. SYSTEMS DIVISION
WASHINGTON, DC 20360

COMMANDER
NAVAIRSYSCOM, CODE-03
DEPT. OF THE NAVY
WASHINGTON, DC 20361

COMMANDER
EARTH & PLANETARY SCIENCES
CODE 3918, NAVAL WEAPONS CENTER
CHINA LAKE, CA 93555

DIRECTOR
NAVY SCIENCE ASST. PROGRAM
NAVSURFWEACEN, WHITE OAKS
SILVER SPRING, MD 20910

COMMANDER
PACMISTESTCEN
CODE 3250
PT. MUGU, CA 93042

NAVAL POSTGRADUATE SCHOOL
DEPT. OF METEOROLOGY
MONTEREY, CA 93940

NAVAL POSTGRADUATE SCHOOL
DEPT. OF OCEANOGRAPHY
MONTEREY, CA 93940

NAVAL POSTGRADUATE SCHOOL
LIBRARY
MONTEREY, CA 93940

COMMANDING OFFICER
NAVEDTRAPRODEVCEN
PD 10/AGS
PENSACOLA, FL 32509

COMMANDING OFFICER
U.S. MARINE CORPS AIR STATION
ATTN: WEATHER SERVICE OFFICE
(HELICOPTER)
FPO SEATTLE 98772

COMMANDING OFFICER
U.S. MARINE CORPS AIR STATION
ATTN: WEATHER SERVICE OFFICE
FPO SEATTLE 98764

COMMANDING OFFICER
MCAS (HELICOPTER)
HQRON OPERATIONS DEPT.
ATTN: WEATHER SERVICE DIV.
JACKSONVILLE, NC 28545

COMMANDER
AWS/DN
SCOTT AFB, IL 62225

USAFETAC/TS
SCOTT AFB, IL 62225

3350TH TECHNICAL TRNG GRP
TTGU-W/STOP 623
CHANUTE AFB, IL 61868

AFGL/LY
HANSCOM AFB, MA 01731

5WW/DN
LANGLEY AFB, VA 23665

OFFICER IN CHARGE
SERVICE SCHOOL COMMAND
DET. CHANUTE/STOP 62
CHANUTE AFB, IL 61868

1ST WEATHER WING (DON)
HICKAM AFB, HI 96853

DET 4 HQ AWS/CC
APO SAN FRANCISCO 96334

DET 5 1WW/CC
APO SAN FRANCISCO 96274

DET 8, 30 WS
APO SAN FRANCISCO 96239

DET 17, 30 WS
APO SAN FRANCISCO 96328

DET 18, 30 WS
APO SAN FRANCISCO 96301

HQ SAC/DOWA
OFFUTT AFB, NE 68113

AFOSR/NC
BOLLING AFB
WASHINGTON, DC 20332

CHIEF
HQ 1ST WEATHER WING (MAC)
AEROSPACE SCIENCES BRANCH
HICKAM AFB, HI 96853

DIRECTOR
TECH. INFORMATION CENTER
ATTN: LIBRARY BRANCH
U.S. ARMY ENGINEERS WATERWAYS
EXPERIMENT STATION
VICKSBURG, MS 39180

ENGINEER TOPOGRAPHIC LABS
ATTN: ETL-GS-A
FT. BELVOIR, VA 22060

DIRECTOR
DEFENSE TECH. INFO. CENTER
CAMERON STATION
ALEXANDRIA, VA 22314

DIRECTOR
OFFICE OF ENV. & LIFE SCIENCES
OFFICE OF UNDERSECRETARY OF
DEFENSE FOR RSCH & ENG (E&LS)
RM 3D129, THE PENTAGON
WASHINGTON, DC 20301

CHIEF, MARINE SCIENCE SECTION
U.S. COAST GUARD ACADEMY
NEW LONDON, CT 06320

DIRECTOR
SYSTEMS DEVELOPMENT NWS/NOAA
RM 1216 - THE GRAMAX BLDG.
8060 13TH STREET
SILVER SPRING, MD 20910

NATIONAL METEOROLOGICAL CENTER
DEVELOPMENT DIV., NWS/NOAA
WORLD WEATHER BLDG. W32, RM 204
WASHINGTON DC 20233

ACQUISITIONS SECTION IRDB-D823
LIBRARY & INFO SERV DIV NOAA
6009 EXECUTIVE BLVD
ROCKVILLE, MD 20852

CHIEF, MARINE & EARTH SCIENCES
LIBRARY, NOAA
DEPARTMENT OF COMMERCE
ROCKVILLE, MD 20852

FEDERAL COORDINATOR FOR
METEORO. SERVICES &
SUPPORTING RESEARCH
6010 EXECUTIVE BLVD.
ROCKVILLE, MD 20852

DIRECTOR
OFFICE OF PROGRAMS RX3
NOAA RESEARCH LAB
BOULDER, CO 80302

DIRECTOR
NATIONAL HURRICANE CENTER, NOAA
UNIV. OF MIAMI BRANCH
CORAL GABLES, FL 33124

NATIONAL WEATHER SERVICE
WORLD WEATHER BLDG., RM 307
5200 AUTH ROAD
CAMP SPRINGS, MD 20023

NATIONAL CLIMATIC CENTER
ATTN: L. PRESTON D542X2
FEDERAL BLDG. - LIBRARY
ASHEVILLE, NC 28801

NATIONAL WEATHER SERVICE
ATTN: WFE3, EASTERN REGION
585 STEWART AVE.
GARDEN CITY, NY 11530

CHIEF, SCIENTIFIC SERVICES
NWS, SOUTHERN REGION
NOAA, ROOM 10E09
819 TAYLOR STREET
FT. WORTH, TX 76102

CHIEF, SCIENTIFIC SERVICES
NWS, PACIFIC REGION
P.O. BOX 50027
HONOLULU, HI 96850

NOAA RESEARCH FACILITIES CENTER
P.O. BOX 520197
MIAMI, FL 33152

NATIONAL WEATHER SERVICE
FORECAST OFFICE
ATTN: METEOROLOGIST OFFICE
TECHNOLOGY II, NOAA
NEW YORK UNIVERSITY
BRONX, NY 10453

CIRECTOR
ATLANTIC OCEANOGRAPHIC &
METEOR. LABS
15 RICKENBACKER CAUSEWAY
VIRGINIA KEY
MIAMI, FL 33149

DIRECTOR
GEOPHYSICAL FLUID DYNAMICS LAB
NOAA, PRINCETON UNIV.
P.O. BOX 308
PRINCETON, NJ 08540

NATIONAL MARINE FISHERIES SERV.
OCEAN CLIMATOLOGY PROJECT
SOUTHWEST FISHERIES CENTER
P.O. BOX 271
LA JOLLA, CA 92037

SF-NOAA LIAISON MANAGER
NASA-JOHNSON SPACE CENTER
ATTN: DR. MICHAEL HELFERT
HOUSTON, TX 77058

METEOROLOGIST IN CHARGE
WEATHER SERVICE FORECAST
OFFICE, NOAA
660 PRICE AVE.
REDWOOD CITY, CA 94063

DIRECTOR
CENTRAL PACIFIC HURRICANE CENTER
NWS, NOAA
HONOLULU, HI 96819

DIRECTOR
INTERNATIONAL AFFAIRS OFFICE
ATTN: MR. N. JOHNSON, NOAA
6010 EXECUTIVE BLVD.
ROCKVILLE, MD 20852

METEOROLOGIST IN CHARGE
WEATHER SERVICE FORECAST OFFICE
NOAA
HONOLULU INTERNATIONAL AIRPORT
HONOLULU, HI 96819

DIRECTOR
NATIONAL SCIENCE FOUNDATION
DIV. OF ATMOS. SCIENCES, RM 644
1800 G. STREET, NW
WASHINGTON, DC 20550

LABORATORY FOR ATMOS. SCIENCES
NASA GODDARD SPACE FLIGHT CENTER
GREENBELT, MD 20771

PRELIMINARY SYSTEMS DESIGN GRP.
NASA GODDARD SPACE FLIGHT CENTER
GREENBELT, MD 20771

EXECUTIVE SECRETARY
CAO SUBCOMMITTEE ON ATMOS. SCIENCES
NATIONAL SCIENCE FOUNDATION, RM 510
1800 G. STREET NW
WASHINGTON, DC 20550

FEDERAL EMERGENCY MANAGEMENT
AGENCY (FEMA)
1725 I STREET NW
WASHINGTON, DC 20472

CHAIRMAN
PENNSYLVANIA STATE UNIV.
503 DEIKE BLDG.
UNIVERSITY PARK, PA 16802

CHAIRMAN
MASSACHUSETTS INSTITUTE OF TECH.
DEPT. OF METEOROLOGY
CAMBRIDGE, MA 02139

ATMOSPHERIC SCIENCES DEPT.
UNIVERSITY OF CHICAGO
1100 E. 57TH STREET
CHICAGO, IL 60637

UNIVERSITY OF WASHINGTON
ATMOSPHERIC SCIENCES DEPT.
SEATTLE, WA 98195

FLORIDA STATE UNIVERSITY
ENVIRONMENTAL SCIENCES DEPT.
TALLAHASSEE, FL 32306

UNIVERSITY OF HAWAII
DEPT. OF METEOROLOGY
2525 CORREA ROAD
HONOLULU, HI 96822

CHAIRMAN
UNIV. OF WISCONSIN
DEPT. OF METEOROLOGY
1225 WEST DAYTON STREET
MADISON, WI 53706

DIRECTOR
UNIVERSITY OF MIAMI
REMOTE SENSING LAB
P.O. BOX 248003
CORAL GABLES, FL 33124

OREGON STATE UNIVERSITY
ATMOSPHERIC SCIENCES DEPT.
CORVALLIS, OR 97331

CHAIRMAN
UNIVERSITY OF ARIZONA
INSTITUTE OF ATMOS. PHYSICS
TUSCON, AZ 85721

TEXAS A & M UNIVERSITY
DEPT. OF METEOROLOGY
COLLEGE STATION, TX 77843

CHAIRMAN
UNIVERSITY OF UTAH
DEPT. OF METEOROLOGY
SALT LAKE CITY, UT 84112

CHAIRMAN
RUTGERS UNIVERSITY
DEPT. OF METEOROLOGY & PHYSICAL
OCEANO.
P.O. BOX 231
NEW BRUNSWICK, NJ 08903

DIRECTOR OF RESEARCH
INSTITUTE FOR STORM RESEARCH
UNIV. OF ST. THOMAS
3812 MONTROSE BLVD.
HOUSTON, TX 77006

CHAIRMAN
DEPT. OF METEOROLOGY
CALIFORNIA STATE UNIV. SAN JOSE
SAN JOSE, CA 95192

SCRIPPS INSTITUTION OF OCEANO.
LIBRARY, DOCUMENTS/REPORTS SEC.
LA JOLLA, CA 92037

STATE UNIV. OF NEW YORK, ALBANY
ATMOS. SCIENCES DEPT., LIBRARY
400 WASHINGTON AVE.
ALBANY, NY 12222

DIRECTOR
SAN DIEGO STATE UNIVERSITY
CENTER FOR MARINE STUDIES
SAN DIEGO, CA 92182

UNIVERSITY OF MIAMI
R.S.M.A.S. LIBRARY
4600 RICKENBACKER CAUSEWAY
VIRGINIA KEY
MIAMI, FL 33149

HEAD, DEPT. OF ENV. SCIENCES
UNIVERSITY OF VIRGINIA, CLARK HALL
ATTN: R. PIELKE
CHARLOTTESVILLE, VA 22903

CHAIRMAN
DEPT. OF ATMOSPHERIC SCIENCES
UNIVERSITY OF VIRGINIA
CLARK HALL
CHARLOTTESVILLE, VA 22903

ATMOSPHERIC SCIENCES DEPT.
UCLA
405 HILGARD AVE.
LOS ANGELES, CA 90024

DEPT. OF ATMOS. SCIENCES LIBRARY
COLORADO STATE UNIVERSITY
FOOTHILLS CAMPUS
FT. COLLINS, CO 80523

EASTERN AIR LINES, INC.
METEOROLOGY DEPT.
MIAMI INTERNATIONAL AIRPORT
MIAMI, FL 33148

CENTER FOR THE ENVIRONMENT & MAN, INC., RESEARCH LIBRARY
275 WINDSOR STREET
HARTFORD, CT 06120

THE WALTER A. BOHAN CO.
2026 OAKTON STREET
PARK RIDGE, IL 60068

LIBRARY
THE RAND CORPORATION
1700 MAIN STREET
SANTA MONICA, CA 90406

MANAGER
METEOROLOGICAL SERVICES
PAN AMERICAN WORLD AIRWAYS
HANGAR 14, JFK INTERNATIONAL AIRPORT
JAMAICA, NY 11430

CONTROL DATA CORP.
METEOROLOGY DEPT. RESEARCH DIV.
2800 E. OLD SHAKOPEE RD.
BOX 1249
MINNEAPOLIS, MN 55440

PRESIDENT
GEOATMOSPHERICS CORP.
BOX 177
LINCOLN, MA 01773

LABORATORY OF CLIMATOLOGY
ROUTE 1
CENTERTON
ELMER, NJ 08318

DIRECTOR OF METEOROLOGY
TRANSWORLD AIRLINES, INC.
HANGAR 12 - RM 235
J.F. K. INTERNATIONAL AIRPORT
JAMAICA, NY 11430

LIBRARY
GULF COAST RESEARCH LAB
OCEAN SPRINGS, MS 39564

SEA USE COUNCIL
1101 SEATTLE TOWER
SEATTLE, WA 98101

OCEAN DATA SYSTEMS, INC.
2460 GARDEN ROAD
MONTEREY, CA 93940

SYSTEMS & APPLIED SCI. CORP.
ATTN: LIBARY, SUITE 500
6811 KENILWORTH AVE.
RIVERDALE, MD 20840

NAUTILUS PRESS, INC.
WEATHER & CLIMATE REPORT
1056 NATIONAL PRESS BLDG.
WASHINGTON, DC 20045

UNIVERSAL MARINE, INC.
8222 TRAVELAIR ST.
HOUSTON, TX 77061

OCEANROUTES, INC.
3260 HILLVIEW AVE.
PALO ALTO, CA 94304

THE EXECUTIVE DIRECTOR
AMERICAN METEOROLOGICAL SOCIETY
45 BEACON STREET
BOSTON, MA 02108

AMERICAN MET. SOCIETY
METEOROLOGICAL & GEOASTRO-PHYSICAL ABSTRACTS
P.O. BOX 1736
WASHINGTON, DC 20013

DIRECTOR, JTWC
BOX 17
FPO SAN FRANCISCO 96630

WORLD METEOROLOGICAL ORG.
ATS DIVISION (ATTN: N. SUZUKI)
CH-1211, GENEVA 20,
SWITZERLAND

LIBRARY, CSIRO DIV.
ATMOSPHERIC PHYSICS
STATION STREET
ASPENDALE, 3195
VICTORIA, AUSTRALIA

LIBRARIAN
METEOROLOGY DEPT.
UNIV. OF MELBOURNE
PARKVILLE, VICTORIA 3052
AUSTRALIA

BUREAU OF METEOROLOGY
ATTN: LIBRARY
BOX 1289K, GPO
MELBOURNE, VIC, 3001
AUSTRALIA

JAMES COOK UNIV. OF NORTH QUEENSLAND
DEPT. OF GEOGRAPHY
TOWNSVILLE Q4811
AUSTRALIA

UNIV. OF NEW SOUTH WALES
WATER RESEARCH LAB
KING ST., MANLY VALE
NSW 2093 AUSTRALIA

LIBRARY
ATMOSPHERIC ENVIRONMENT SERVICE.
4905 DUFFERIN STREET
DOWNSVIEW M3H 5T4
ONTARIO, CANADA

DIRECTOR OF METEOROLOGY & OCEANOGRAPHY
NATIONAL DEFENSE HDQ
OTTAWA, ONTARIO K1A 0K2
CANADA

METOC CENTRE
MARITIME FORCES PACIFIC HDQ
FORCES MAIL OFFICE
VICTORIA, BRITISH COLUMBIA
V0S-1B0 CANADA

METEOROLOGICAL OFFICE LIBRARY
LONDON ROAD
BRACKNELL, BERKSHIRE
RG 12 2SZ ENGLAND

DEPT. OF METEOROLOGY
UNIV. OF READING
2 EARLYGATE, WHITEKNIGHTS
READING RG6 2AU
ENGLAND

EUROPEAN CENTRE FOR MEDIUM RANGE WEATHER FORECASTS
SHINFIELD PARK, READING
BERKSHIRE RG29AX, ENGLAND

LIBRARY
FINNISH METEOROLOGICAL INSTITUTE
BOX 503
SF-00101 HELSINKI 10
FINLAND

METEOROLOGIE NATIONALE
SMM/DOCUMENTATION
2, AVENUE RAPP
75340 PARIS CEDEX 07
FRANCE

DIRECTION DE LA METEOROLOGIE MN/RE
ATTN: J. DETTWILLER
77 RUE DE SEVRES
92106 BOULOGNE-BILLANCOURT CEDEX
FRANCE

DEUTSCHER HYDROGRAPHISCHES INSTITUT
ATTN: DIRECTOR
TAUSCHSTELLE POSTFACH 220
D2000 HAMBURG 4
FEDERAL REPUBLIC OF GERMANY

DIRECTOR
ROYAL OBSERVATORY
NATHAN ROAD, KOWLOON
HONG KONG, B.C.C.

THE DIRECTOR
INDIAN INSTITUTE OF TROP. METEOR.
RAMDURG HOUSE, PUNE 411-005
INDIA

NATIONAL INSTITUTE OF OCEANOGRAPHY
REGIONAL CENTRE, P.B. 1913
COCHIN-682018
INDIA

DIRECTOR GENERAL
METEOROLOGICAL DEPT.
GOVERNMENT OF INDIA
NEW DELHI, 3 INDIA

DEPT. OF METEOROLOGY
ANDHRA UNIVERSITY
WALTAIR, INDIA 530-003

DIRECTOR
METEOROLOGICAL & GEOPHYSICAL SERV.
C/O DJALAN ARIEF RACHMAN HAKIM 3
DJAKARTA, INDONESIA

DIRECTOR
ISRAEL METEOROLOGICAL SERVICE
P.O. BOX 25
BET DAGEN 50200, ISRAEL

LIBRARY
METEOROLOGICAL RESEARCH INSTITUTE
KOENJI-KITA, SUGINAMI
TOKYO 166, JAPAN

TYPHOON RESEARCH LABORATORY
ATTN: LIBRARIAN
METEOROLOGICAL RESEARCH INSTITUTE
1-1 NAGAMINE, YATABE-MACHI,
TSUKUBA-GUN,
IBARAKI-KEN, 305, JAPAN

OCEAN RESEARCH INSTITUTE LIBRARY
UNIVERSITY OF TOKYO
15-1, 1-CHOME
MINAMIDAI, NAKANO-KU
TOKYO, JAPAN

MARITIME METEOROLOGY DIV.
JAPAN METEOROLOGICAL AGENCY
OTE-MACHI 1-3-4 CHIYODA-KU
TOKYO, JAPAN

HYDROGRAPHI DEPT.
MARITIME SAFETY AGENCY
3-1, Tsukiji 5-CHOME
CHUO-KU, TOKYO

JAPAN METEOROLOGICAL AGENCY
3-4, OTEMACHI 1-CHOME,
CHIYODA-KU
TOKYO 100, JAPAN

METEOROLOGICAL INSTITUTE
FACULTY OF SCIENCE
KYOTO UNIVERSITY
ATTN: DR. R. YAMAMOTO
SAKYO, KYOTO 606, JAPAN

WEATHER CENTRAL SERVICE SQ.
JASDF
FUCHU, TOKYO

DIRECTOR GENERAL
MALAYSIAN METEOROLOGICAL SERVICE
JALAN SULTAN
PETALING JAYA
SELANGOR, WEST MALAYSIA

KONINKLIJK NEDERLANDS
METEOROLOGISCH INSTITUUT
POSTBUS 201
3730 AE DEBILT
NETHERLANDS

BUREAU HYDROGRAFIE DER
KONINKLIJKE MARINE
AFD MILOC/METEO
BADHUISWEG 171
DEN HAAG, NETHERLANDS

LIBRARIAN
NEW ZEALAND METEOROLOGICAL SERV.
P.O. BOX 722
WELLINGTON, NEW ZEALAND

THE LIBRARIAN
NEW ZEALAND OCEANOGRAPHIC
INSTITUTE
P.O. BOX 12-346
WELLINGTON NORTH, NEW ZEALAND

DEPT. OF METEOROLOGY
COLLEGE OF ARTS & SCIENCES
UNIV. OF THE PHILIPPINES
DILMAN, QUEZON CITY 3004
PHILIPPINES

TECHNICAL LIBRARY
WEATHER BUREAU
DEPT. OF NATIONAL DEFENSE
LUNGSOD NG QUEZON
QUEZON, PHILIPPINES

NATIONAL WEATHER SERVICE
PHILIPPINE ATMOSPHERIC
GEOPHYSICAL & ASTRONOMICAL
SERVICES ADMIN (PAGASA)
1424 QUEZON AVE.
QUEZON CITY, METRO MANILA
PHILIPPINES

DIRECTOR
TYPHOON MODERATION RSCH &
DEVELOPMENT OFFICE (PAGASA)
MINISTRY OF NATIONAL DEFENSE
1424 QUEZON AVE.
QUEZON CITY, PHILIPPINES

COORDINATOR
ESCAP/WMO TYPHOON COMMITTEE
SECRETARIAT
C/O UNDP
MANILA, PHILIPPINES

LIBRARY
UNIV. OF STOCKHOLM
DEPT. OF METEOROLOGY
ARRHENIUS LABORATORY
S-106 91 STOCKHOLM, SWEDEN

COORDINATOR, NATIONAL ATMOSPHERIC
RESEARCH PROGRAM
INSTITUTE OF PHYSICS
ACADEMIA SINICA
TAIPEI, TAIWAN

CENTRAL WX BUREAU
64, KUNG YUAN RD
TAIPEI, TAIWAN 100

NATIONAL TAIWAN UNIVERSITY
DEPT. OF ATMOSPHERIC SCIENCE
TAIPEI, TAIWAN 107

DEPUTY DIRECTOR-GENERAL
THAILAND METEOROLOGICAL DEPT.
MINISTRY OF COMMUNICATIONS
BANGKOK, THAILAND